EUROPEAN ORGANIZATION FOR NUCLEAR RESEARCH (CERN)

Searches for long-lived charged particles in pp collisions at $\sqrt{s} =$ 7 and 8 TeV

The CMS Collaboration*

Abstract

Results of searches for heavy stable charged particles produced in pp collisions at $\sqrt{s} = 7$ and 8 TeV are presented corresponding to an integrated luminosity of $5.0\,\mathrm{fb}^{-1}$ and $18.8\,\mathrm{fb}^{-1}$, respectively. Data collected with the CMS detector are used to study the momentum, energy deposition, and time-of-flight of signal candidates. Leptons with an electric charge between $e/3$ and $8e$, as well as bound states that can undergo charge exchange with the detector material, are studied. Analysis results are presented for various combinations of signatures in the inner tracker only, inner tracker and muon detector, and muon detector only. Detector signatures utilized are long time-of-flight to the outer muon system and anomalously high (or low) energy deposition in the inner tracker. The data are consistent with the expected background, and upper limits are set on the production cross section of long-lived gluinos, scalar top quarks, and scalar τ leptons, as well as pair produced long-lived leptons. Corresponding lower mass limits, ranging up to $1322\,\mathrm{GeV}/c^2$ for gluinos, are the most stringent to date.

*See Appendix A for the list of collaboration members

1 Introduction

Many extensions of the standard model (SM) include heavy, long-lived, charged particles that have speed v significantly less than the speed of light c [1–3] or charge Q not equal to the elementary positive or negative charge $\pm 1e$ [4–8], or both. With lifetimes greater than a few nanoseconds, these particles can travel distances comparable to the size of modern detectors and thus appear to be stable. These particles, generically referred to as heavy stable charged particles (HSCP), can be singly charged ($|Q| = 1e$), fractionally charged ($|Q| < 1e$), or multiply charged ($|Q| > 1e$). Without dedicated searches, HSCPs may be misidentified or even completely missed, as particle identification algorithms at hadron collider experiments generally assume signatures appropriate for SM particles, e.g., $v \approx c$ and $Q = 0$ or $\pm 1e$. Additionally, some HSCPs may combine with SM particles to form composite objects. Interactions of these composite objects with the detector may change their constituents and possibly their electric charge, further limiting the ability of standard algorithms to identify them.

For HSCP masses greater than $100\,\mathrm{GeV}/c^2$, a significant fraction of particles produced at the Large Hadron Collider (LHC) have β ($\equiv v/c$) values less than 0.9. These HSCPs can be identified by their longer time-of-flight (TOF) to outer detectors or their anomalous energy loss ($\mathrm{d}E/\mathrm{d}x$). The $\mathrm{d}E/\mathrm{d}x$ of a particle depends on both its electric charge (varying as Q^2) and its β. The dependence of $\mathrm{d}E/\mathrm{d}x$ on these variables is described by the Bethe-Bloch formula [9]. This dependence can be seen in Fig. 1, which shows a $\mathrm{d}E/\mathrm{d}x$ estimate versus momentum for tracks from data and Monte Carlo (MC) simulations of HSCP signals with various charges. In the momentum range of interest (10–1000 GeV/c), SM charged particles have a relatively flat ionization energy loss and β values very close to one. Searching for candidates with long time-of-flight or large $\mathrm{d}E/\mathrm{d}x$ gives sensitivity to massive particles with $|Q| = 1e$, particles with $|Q| > 1e$, and low-momentum particles with $|Q| < 1e$. On the other hand, searching for candidates with lower $\mathrm{d}E/\mathrm{d}x$ yields sensitivity to high-momentum particles with $|Q| < 1e$.

Previous collider searches for HSCPs have been performed at LEP [10–13], HERA [14], the Tevatron [15–18], and the LHC [19–26]. The results from such searches have placed important bounds on beyond the standard model (BSM) theories [27, 28], such as lower limits on the mass of gluinos, scalar top quarks (stops), and pair-produced scalar τ leptons (staus) at 1098, 737, and 223 GeV/c^2, respectively. Presented here are several searches for singly, fractionally, and multiply charged HSCPs using data collected with the Compact Muon Solenoid (CMS) detector during the 2011 ($\sqrt{s} = 7\,\mathrm{TeV}$, $5.0\,\mathrm{fb}^{-1}$) and 2012 ($\sqrt{s} = 8\,\mathrm{TeV}$, $18.8\,\mathrm{fb}^{-1}$) data taking periods.

2 Signal benchmarks

The searches presented here are sensitive to a wide variety of signals of new charged massive particles. Several BSM models are used to benchmark the sensitivity. The HSCPs can be classified as either *lepton-like* or *hadron-like*. Lepton-like HSCPs interact primarily through the electromagnetic force, while hadron-like HSCPs additionally interact through the strong force and form bound states with SM quarks (or gluons) called *R*-hadrons [29]. The *R*-hadrons can be charged or neutral. Strong interactions between the SM quarks and detector material increase energy loss and can lead to charge exchange, e.g., conversion of charged *R*-hadrons into neutral ones (and vice-versa). There is some uncertainty in the modeling of *R*-hadrons' strong interactions with detector material. For this analysis, two separate models are considered: (1) the model described in Refs. [30, 31], referred to as the cloud model, and (2) a model in which any strong interaction results in a neutral *R*-hadron [32], referred to as the charge-suppressed
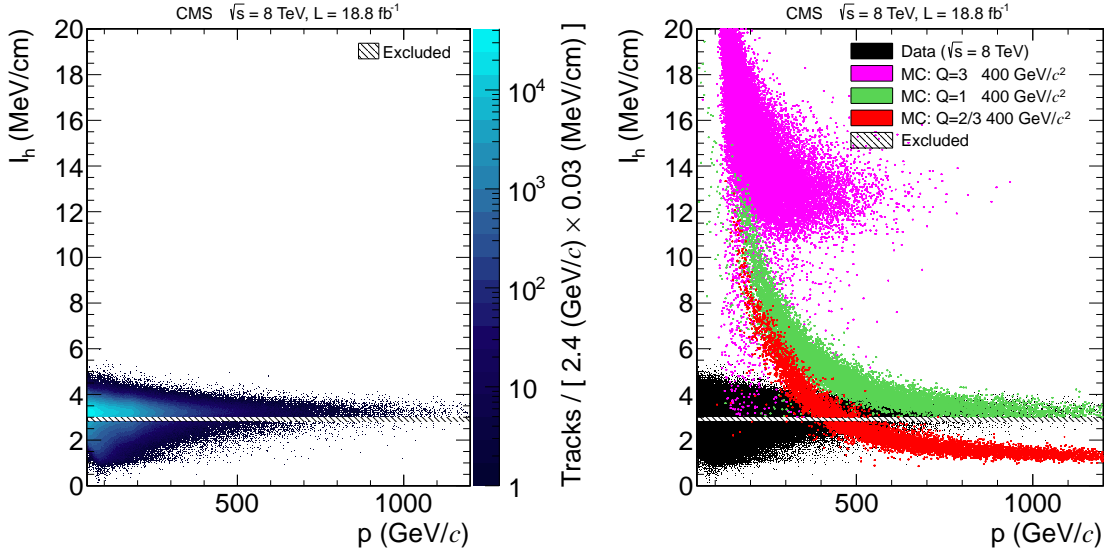
Figure 1: Distribution of I_h, a dE/dx estimator that is defined in Section 3.1, versus particle momentum for $\sqrt{s} = 8$ TeV data (left) and also including MC simulated HSCP candidates of different charges (right). Tracks with $2.8 \leq I_h \leq 3.0$ MeV/cm are excluded by preselection requirements, as discussed in Section 4.

model. The cloud model envisions the R-hadron as composed of a spectator HSCP surrounded by a cloud of colored, light constituents. The charge-suppressed model results in essentially all R-hadrons being neutral by the time they enter the muon system. For each of the models considered, particle interactions with the CMS apparatus and detector response are simulated using GEANT4 v9.2 [33, 34]. To produce the effect of multiple interactions per bunch crossing (pileup), simulated minimum bias events are overlaid with the primary collision.

The minimal gauge-mediated supersymmetry breaking (GMSB) model [35] predicts the gravitino to be the lightest supersymmetric particle (LSP) and allows for the next-to-lightest supersymmetric particle (NLSP) to be long-lived because of the weakness of the gravitational coupling, which governs the decay of the NLSP to the LSP. For this analysis the NLSP is taken to be a lepton-like stau ($\widetilde{\tau}_1$) with an assumed lifetime that exceeds the time-of-flight through the CMS detector. For $\sqrt{s} = 7$ (8) TeV simulation, PYTHIA v6.422 (v6.426) [36] is used to model both Drell–Yan production of a $\widetilde{\tau}_1$ pair (direct pair-production) and production of heavier supersymmetric particles whose decay chains lead to indirect stau production. Events with $\widetilde{\tau}_1$ masses in the range 100–557 GeV/c^2 are generated using line 7 of the "Snowmass Points and Slopes" benchmarks [37]. They correspond to $N = 3$ chiral SU(5) multiplets added to the theory at a scale F from 60 to 360 TeV [35] depending on the $\widetilde{\tau}_1$ mass, and an effective supersymmetry-breaking scale of $\Lambda = F/2$. All points have a value of 10 for the ratio of neutral Higgs field vacuum expectation values ($\tan\beta$), a positive sign for the Higgs-Higgsino mass parameter (sgn(μ)), and a value of 10^4 for the ratio of the gravitino mass to the value it would have if the only supersymmetry-breaking scale were that in the messenger sector (c_{grav}). The particle mass spectrum and the decay table were produced with the program ISASUGRA version 7.69 [38]. Theoretical production cross sections (σ_{th}) for staus are calculated at next-to-leading order (NLO) with PROSPINO v2.1 [39]. Compared to the previous publication [24], the theoretical NLO cross section used for the indirect production of staus also includes processes involving pairs of neutralinos/charginos.

R-hadron signals from gluino ($\widetilde{g}$) and scalar top ($\widetilde{t}_1$) pair production are studied using PYTHIA

v6.442 (v8.153) [36, 40] for $\sqrt{s} = 7$ (8) TeV generation. Stop pair production is modeled for masses in the range 100–1000 GeV/c^2. For $\widetilde{g}$ production, split supersymmetry [41, 42] is modeled by setting the squark masses to greater than 10 TeV/c^2 and generating $\widetilde{g}$ masses of 300–1500 GeV/c^2. The fraction f of gluinos hadronizing into $\tilde{g}$-gluon bound states is unknown. These neutral states would not leave a track in the inner detectors. Therefore, several scenarios are considered for the singly charged analysis: $f = 0.1$, 0.5, and 1.0. In the extreme case where $f = 1.0$, R-hadrons are always neutral in the inner tracker, but a fraction of them may interact with the detector material and be electrically charged during their passage through the muon system. Gluino and scalar top pair production cross sections are calculated at NLO plus next-to-leading logarithmic (NLL) accuracy with PROSPINO v2.1 [43–50].

The last of the signal samples studied is the modified Drell–Yan production of long-lived leptons. In this scenario, new massive spin-1/2 particles may have an electric charge different than $|Q| = 1e$ and are neutral under $SU(3)_C$ and $SU(2)_L$; therefore they couple only to the photon and the Z boson via $U(1)$ couplings [51]. Signal samples are simulated using PYTHIA v6.422 (v6.426) [36] for $\sqrt{s} = 7$ (8) TeV. The analysis uses simulations of $|Q| = e/3$ and $2e/3$ for masses of 100–600 GeV/c^2, of $|Q|$ ranging from $1e$ to $6e$ for masses of 100–1000 GeV/c^2, and of $|Q| = 7e$ and $8e$ for masses of 200–1000 GeV/c^2.

The CTEQ6L1 parton distribution functions (PDF) [52] are used for the sample generation.

3 The CMS detector

The CMS experiment uses a right-handed coordinate system, with the origin at the nominal interaction point, the x axis pointing to the center of the LHC ring, the y axis pointing up (perpendicular to the plane of the LHC ring), and the z axis along the counterclockwise-beam direction. The polar angle θ is measured from the positive z axis and the azimuthal angle ϕ in the x-y plane. The pseudorapidity is given by $\eta = -\ln[\tan(\theta/2)]$.

The central feature of the CMS apparatus is a superconducting solenoid of 6 m internal diameter. Within the field volume are a silicon pixel and strip tracker, a lead tungstate crystal electromagnetic calorimeter, and a brass and scintillator hadron calorimeter. Muons are measured in gas-ionization detectors embedded in the steel flux-return yoke of the magnet. Extensive forward calorimetry complements the coverage provided by the barrel and endcap detectors. The inner tracker measures charged particles within the pseudorapidity range $|\eta| < 2.5$. It consists of 1440 silicon pixel and 15 148 silicon strip detector modules and is located in the 3.8 T field of the solenoid. The inner tracker provides a transverse momentum (p_{T}) resolution of about 1.5% for 100 GeV/c particles. Muons are measured in the pseudorapidity range $|\eta| < 2.4$, with detection planes made using three technologies: drift tubes (DT), cathode strip chambers (CSC), and resistive plate chambers (RPC). The muon system extends out to eleven meters from the interaction point in the z direction and seven meters radially. Matching tracks in the muon system to tracks measured in the silicon tracker results in a transverse momentum resolution between 1 and 5%, for p_{T} values up to 1 TeV/c. The first level (L1) of the CMS trigger system, composed of custom hardware processors, uses information from the calorimeters and muon detectors to select events of interest. The high level trigger (HLT) processor farm further decreases the event rate from around 100 kHz to around 300 Hz for data storage. A more detailed description of the CMS detector can be found in Ref. [53].

3.1   The dE/dx measurements

As in Ref. [19], dE/dx for a track is estimated as:

$$I_h = \left(\frac{1}{N} \sum_i c_i^{-2} \right)^{-1/2},$$

(1)

where N is the number of measurements in the silicon-strip detectors and c_i is the energy loss per unit path length in the sensitive part of the silicon detector of the ith measurement; I_h has units MeV/cm. In addition, two modified versions of the Smirnov–Cramer–von Mises [54, 55] discriminator, I_{as} (I'_{as}), are used to separate SM particles from candidates with large (small) dE/dx. The discriminator is given by:

$$I_{as}^{(\prime)} = \frac{3}{N} \times \left(\frac{1}{12N} + \sum_{i=1}^{N} \left[P_i^{(\prime)} \times \left(P_i^{(\prime)} - \frac{2i-1}{2N} \right)^2 \right] \right),$$

(2)

where P_i (P'_i) is the probability for a minimum ionizing particle (MIP) to produce a charge smaller (larger) or equal to that of the ith measurement for the observed path length in the detector, and the sum is over the measurements ordered in terms of increasing $P_i^{(\prime)}$.

As in Ref. [19], the mass of a $|Q| = 1e$ candidate particle is calculated based on the relationship:

$$I_h = K \frac{m^2}{p^2} + C,$$

(3)

where the empirical parameters $K = 2.559 \pm 0.001\,\text{MeV} \cdot c^2/\text{cm}$ and $C = 2.772 \pm 0.001\,\text{MeV/cm}$ are determined from data using a sample of low-momentum protons in a minimum-bias dataset.

The number of silicon-strip measurements associated with a track, 15 on average, is sufficient to ensure good dE/dx and mass resolutions.

3.2   Time-of-flight measurements

As in Ref. [24], the time-of-flight to the muon system can be used to discriminate between $\beta \approx 1$ particles and slower candidates. The measured time difference (δ_t) of a hit relative to that expected for a $\beta = 1$ particle can be used to determine the particle $1/\beta$ via the equation:

$$1/\beta = 1 + \frac{c\delta_t}{L},$$

(4)

where L is the flight distance from the interaction point. The track $1/\beta$ value is calculated as the weighted average of the $1/\beta$ measurements from the DT and CSC hits associated with the track. A description of how the DT and CSC systems measure the time of hits is given below.

As tubes in consecutive layers of DT chambers are staggered by half a tube, a typical track passes alternatively to the left and to the right of the sensitive wires in consecutive layers. The position of hits is inferred from the drift time of the ionization electrons assuming the hits come from a prompt muon. For a late arriving HSCP, the delay will result in a longer drift time being attributed, so hits drifting left will be to the right of their true position while hits drifting right will be to the left. The DT measurement of δ_t then comes from the residuals of a straight line fit to the track hits in the chamber. Only phi-projections from the DT chambers are used for this purpose. The weight for the ith DT measurement is given by:

$$w_i = \frac{(n-2)}{n} \frac{L_i^2}{c^2 \sigma_{DT}^2},$$

(5)

where n is the number of ϕ projection measurements found in the chamber from which the measurement comes and $\sigma_{DT} = 3$ ns is the time resolution of the DT measurements. The factor $(n-2)/n$ accounts for the fact that residuals are computed using two parameters of a straight line determined from the same n measurements (the minimum number of hits in a DT chamber needed for a residual calculation is $n = 3$). Particles passing through the DTs have on average 16 time measurements.

The CSC measurement of δ_t is found by measuring the arrival time of the signals from both the cathode strips and anode wires with respect to the time expected for prompt muons. The weight for the ith CSC measurement is given by:

$$w_i = \frac{L_i^2}{c^2 \sigma_i^2}, \tag{6}$$

where σ_i, the measured time resolution, is 7.0 ns for cathode strip measurements and 8.6 ns for anode wire measurements. Particles passing through the CSCs have on average 30 time measurements, where cathode strip and anode wire measurements are counted separately.

The uncertainty ($\sigma_{1/\beta}$) on $1/\beta$ for the track is found via the equation:

$$\sigma_{1/\beta} = \sqrt{\sum_{i=1}^{N} \frac{(1/\beta_i - \overline{1/\beta})^2 \times w_i}{N-1}}, \tag{7}$$

where $\overline{1/\beta}$ is the average $1/\beta$ of the track and N is the number of measurements associated with the track.

Several factors including the intrinsic time resolution of the subsystems, the typical number of measurements per track, and the distance from the interaction point lead to a resolution of about 0.065 for $1/\beta$ in both the DT and CSC subsystems over the full η range.

4 Data selection

Multiple search strategies are used to separate signal from background depending on the nature of the HSCP under investigation.

- For singly charged HSCPs,
  - the "tracker+TOF" analysis requires tracks to be reconstructed in the inner tracker and the muon system,
  - the "tracker-only" analysis only requires tracks to be reconstructed in the inner tracker, and
  - the "muon-only" analysis only requires tracks to be reconstructed in the muon system.
- For fractionally charged HSCPs, the "fractionally charged" ($|Q| < 1e$) analysis only requires tracks to be reconstructed in the inner tracker and to have a dE/dx smaller than SM particles.
- For multiply charged HSCPs, the "multiply charged" ($|Q| > 1e$) analysis requires tracks to be reconstructed in the inner tracker and the muon system. The analysis is optimized for much larger ionization in the detector compared to the tracker+TOF analysis.

HSCP signal events have unique characteristics. For each analysis, the primary background arises from SM particles with random fluctuations in energy deposition/timing or mis-measurement of the energy, timing, or momentum.

The tracker-only and muon-only cases allow for the possibility of charge flipping (charged to neutral or vice versa) within the calorimeter or tracker material. The muon-only analysis is the first CMS search that does not require an HSCP to be charged in the inner tracker. The singly, multiply, and fractionally charged analyses feature different selections, background estimates, and systematic uncertainties. The preselection requirements for the analyses are described below.

All events must pass a trigger requiring either the reconstruction of (i) a muon with high p_T or (ii) large missing transverse energy (E_T^{miss}) defined as the magnitude of the vectorial sum of the transverse momenta of all particles reconstructed by an online particle-flow algorithm [56] at the HLT.

The L1 muon trigger allows for late arriving particles (such as slow moving HSCPs) by accepting tracks that produce signals in the RPCs within either the 25 ns time window corresponding to the interaction bunch crossing or the following 25 ns time window. For the data used in this analysis, the second 25 ns time window is empty of proton-proton collisions because of the 50 ns LHC bunch spacing during the 2011 and 2012 operation.

Triggering on E_T^{miss} allows for some recovery of events with hadron-like HSCPs in which none of the R-hadrons in the event are charged in both the inner tracker and the muon system. The E_T^{miss} in the event arises because the particle-flow algorithm rejects tracks not consistent with a SM particle. This rejection includes tracks reconstructed only in the inner tracker with a track p_T much greater than the matched energy deposited in the calorimeter [57] as would be the case for R-hadrons becoming neutral in the calorimeter, and tracks reconstructed only in the muon system as would be the case for R-hadrons that are initially neutral. Thus, in both cases, only the energy these HSCPs deposit in the calorimeter, roughly 10–20 GeV, will be included in the E_T^{miss} calculation. In events in which no HSCPs are reconstructed as muon candidates, significant E_T^{miss} will result if the vector sum of the HSCPs' momenta is large. The E_T^{miss} trigger will collect these events, allowing for sensitivity to HSCP without a muon-like signature.

For all the analyses, the muon trigger requires $p_T > 40$ GeV/c measured in the inner tracker and the E_T^{miss} trigger requires $E_T^{miss} > 150$ GeV at the HLT. The muon-only analysis uses the same two triggers, and additionally a third trigger that requires both a reconstructed muon segment with $p_T > 70$ GeV/c (measured using only the muon system) and $E_T^{miss} > 55$ GeV. For the first part of the 2012 data (corresponding to an integrated luminosity of 700 pb^{-1}), the requirement was $E_T^{miss} > 65$ GeV. Using multiple triggers in all of the analyses allows for increased sensitivity to HSCP candidates that arrive late in the muon system and to hadron-like HSCPs that are sometimes charged in only one of the inner tracker and muon system and sometimes charged in both. The muon-only analysis uses only $\sqrt{s} = 8$ TeV data as the necessary triggers were not available in 2011.

For the tracker-only analysis, all events are required to have a track candidate in the region $|\eta| < 2.1$ with $p_T > 45$ GeV/c (as measured in the inner tracker). In addition, a relative uncertainty in p_T (σ_{p_T}/p_T) less than 0.25 and a track fit χ^2 per number of degrees of freedom (n_d) less than 5 is required. Furthermore, the magnitudes of the longitudinal (d_z) and transverse (d_{xy}) impact parameters are both required to be less than 0.5 cm. The impact parameters d_z and d_{xy} are both defined with respect to the primary vertex that yields the smallest $|d_z|$ for the candidate track. The requirements on the impact parameters are very loose compared with the

resolutions for tracks ($\sigma(d_{xy,z}) < 0.1$ cm) in the inner tracker. Candidates must pass isolation requirements in the tracker and calorimeter. The tracker isolation requirement is $\Sigma p_T < 50$ GeV/c where the sum is over all tracks (except the candidate's track) within a cone about the candidate track $\Delta R = \sqrt{(\Delta \eta)^2 + (\Delta \phi)^2} < 0.3$ radians. The calorimeter isolation requirement is $E/p < 0.3$ where E is the sum of energy deposited in the calorimeter towers within $\Delta R < 0.3$ (including the candidate's energy deposit) and p is the candidate track momentum reconstructed from the inner tracker. Candidates must have at least two measurements in the silicon pixel detector and at least eight measurements in the combination of the silicon strip and pixel detectors. In addition, there must be measurements in at least 80% of the silicon layers between the first and last measurements on the track. To reduce the rate of contamination from clusters with large energy deposition due to overlapping tracks, a "cleaning" procedure is applied to remove clusters in the silicon strip tracker that are not consistent with passage of only one charged particle (e.g., a narrow cluster with most of the energy deposited in one or two strips). After cluster cleaning, there must be at least six measurements in the silicon strip detector that are used for the dE/dx calculation. Finally, $I_h > 3$ MeV/cm is required.

The tracker+TOF analysis applies the same criteria, but additionally requires a reconstructed muon matched to a track in the inner detectors. At least eight independent time measurements are needed for the TOF computation. Finally, $1/\beta > 1$ and $\sigma_{1/\beta} < 0.07$ are required.

The muon-only analysis uses separate criteria that include requiring a reconstructed track in the muon system with $p_T > 80$ GeV/c within $|\eta| < 2.1$. The relative resolution in p_T is approximately 10% in the barrel region and approaches 30% for $|\eta| > 1.8$ [58]. However, charge flipping by R-hadrons can lead to an overestimate of p_T. The effect is more pronounced for gluinos, where all of the electric charge comes from SM quarks. The measured curvature in the muon system for gluinos is 60–70% smaller than would be expected for a muon with the same transverse momentum. The candidate track must have measurements in two or more DT or CSC stations, and $|d_z|$ and $|d_{xy}| < 15$ cm (calculated using tracks from the muon system and measured relative to the nominal beam spot position rather than to the reconstructed vertex). The requirements on $|d_z|$ and $|d_{xy}|$ are approximately 90% and 95% efficient for prompt tracks, respectively. HSCPs are pair produced and often back-to-back in ϕ but not in η because the collision is in general boosted along the z-axis. On the other hand, cosmic ray muons passing close to the interaction point would pass through the top and bottom halves of CMS, potentially giving the appearance of two tracks back-to-back in both ϕ and η. Often only one of these legs will be reconstructed as a track while the other will leave only a muon segment (an incomplete track) in the detector. To reject cosmic ray muons, candidates are removed if there is a muon segment both with η within ± 0.1 of $-\eta_{cand}$, where η_{cand} is the pseudorapidity of the HSCP candidate, and with $|\delta \phi| > 0.3$ radians, where $\delta \phi$ is the difference in ϕ between the candidate and the muon segment. The $|\delta \phi|$ requirement prevents candidates with small $|\eta|$ from being rejected by their proximity to their own muon segments. Additionally, candidates compatible with vertically downward cosmic ray muons, $1.2 < |\phi| < 1.9$ radians, are rejected. To reject muons from adjacent beam crossings, tracks are removed if their time leaving the interaction point as measured by the muon system is within ± 5 ns of a different LHC beam crossing. This veto makes the background from muons from such crossings negligible while removing very little signal. Finally, the same quality requirements used in the tracker+TOF analysis are applied in the muon-only $1/\beta$ measurement.

The fractionally charged search uses the same preselection criteria as the tracker-only analysis except that I_h is required to be <2.8 MeV/cm. An additional veto on cosmic ray muons rejects candidates if a track with $p_T > 40$ GeV/c is found on the opposite side of the detector ($\Delta R > \pi - 0.3$).

Table 1: Preselection criteria on the inner tracker track used in the various analyses as defined in the text.

	$|Q| < 1e$	tracker+TOF	tracker-only	$|Q| > 1e$
$|\eta|$		<2.1		
p_T (GeV/c)		>45		
d_z and d_{xy} (cm)		<0.5		
$\sigma_{p_\mathrm{T}}/p_\mathrm{T}$		<0.25		
Track χ^2/n_d		<5		
# Pixel hits		>1		
# Tracker hits		>7		
Frac. Valid hits		>0.8		
$\Sigma p_\mathrm{T}^\mathrm{trk}(\Delta R < 0.3)$ (GeV/c)		<50		
# dE/dx measurements		>5		
dE/dx strip shape test		yes		no
$E_\mathrm{cal}(\Delta R < 0.3)/p$		<0.3		–
I_h (MeV/cm)	<2.8		>3.0	
ΔR to another track	$<\pi - 0.3$		–	

Table 2: Preselection criteria on the muon system track used in the various analyses as defined in the text.

	tracker+TOF	$|Q| > 1e$	muon-only
# TOF measurements		>7	
$\sigma_{1/\beta}$		<0.07	
$1/\beta$		>1	
$|\eta|$	–		<2.1
p_T (GeV/c)	–		>80
d_z and d_{xy} (cm)	–		<15
# DT or CSC stations	–		>1
Opp. segment $|\eta|$ difference	–		>0.1
$|\phi|$	–		<1.2 OR >1.9
$|\delta t|$ to another beam crossing (ns)	–		>5

The multiply charged particle search uses the same preselection as the tracker+TOF analysis except that the E/p selection is removed. Furthermore, given that a multiply charged particle might have a cluster shape different from that of a $|Q| = 1e$ particle, the cluster cleaning procedure is not applied for the multiply charged analysis.

The preselection criteria applied on the inner tracker track for the analyses are summarized in Table 1 while the criteria on the muon system track are summarized in Table 2.

5   Background prediction

Candidates passing the preselection criteria (Section 4) are subject to two (or three) additional selection criteria to further improve the signal-to-background ratio. For all of the analyses, results are based upon a comparison of the number of candidates passing the final section criteria with the number of background events estimated from the numbers of events that fail combinations of the criteria.
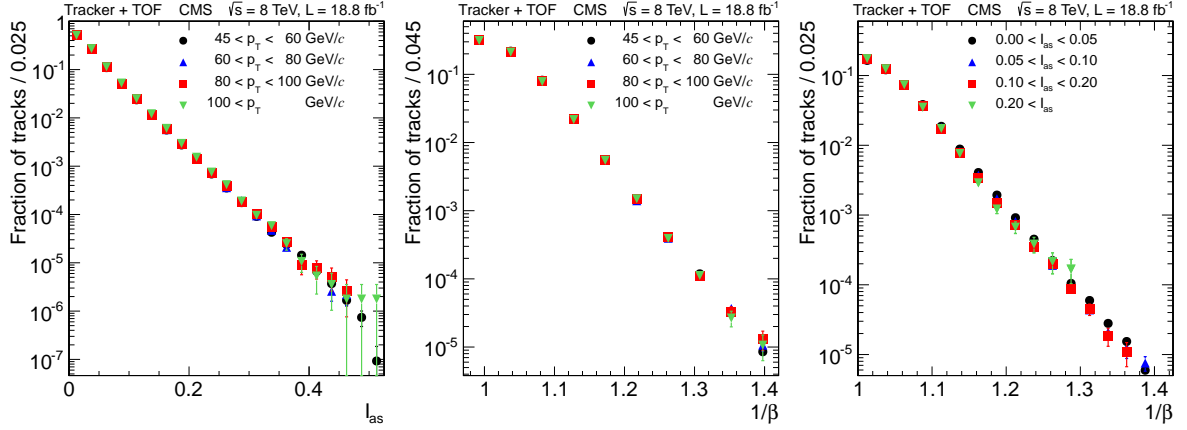
Figure 2: Measured I_{as} (left) and $1/\beta$ (middle) distributions for several p_T ranges and measured $1/\beta$ distributions for several I_{as} ranges (right). Results are for the tracker+TOF selection at $\sqrt{s} = 8$ TeV. The lack of variation of the distributions for different ranges of the other variables demonstrates the lack of strong correlation between $1/\beta$, I_{as}, and p_T.

The background expectation in the signal region, D, is estimated as $D = BC/A$, where B (C) is the number of candidates that fail the first (second) criteria but pass the other one and A is the number of candidates that fail both criteria. The method works if the probability for a background candidate to pass one of the criteria is not correlated with whether it passes the other criteria. The lack of strong correlation between the selection criteria is evident in Fig. 2. Tests of the background prediction (described below) are used to quantify any residual effect and to calculate the systematic error in the background estimate. All tracks passing the preselection enter either the signal region D or one of the control regions that is used for the background prediction.

For the tracker-only analysis, the two chosen criteria are p_T and I_{as}. Threshold values ($p_T > 70$ GeV/c and $I_{as} > 0.4$) are fixed such that failing candidates passing only p_T (I_{as}) fall into the B (C) regions. The B (C) candidates are then used to form a binned probability density function in $I_h(p)$ such that, using the mass determination (Eq. (3)), the full mass spectrum of the background in the signal region D can be predicted. The η distribution of candidates at low dE/dx differs from the distribution of the candidates at high dE/dx. To correct for this effect, events in the C region are weighted such that the η distribution matches that in the B region.

For the tracker+TOF analysis, three criteria are used, p_T, I_{as}, and $1/\beta$, creating eight regions labeled A through H. The final threshold values are selected to be $p_T > 70$ GeV/c, $I_{as} > 0.125$, and $1/\beta > 1.225$. Region D represents the signal region, with events passing all three criteria. The candidates in the A, F, and G regions pass only the $1/\beta$, I_{as}, and p_T criteria, respectively, while the candidates in the B, C, and H regions fail only the p_T, I_{as}, and $1/\beta$ criteria, respectively. The E region fails all three criteria. The background estimate can be made from several different combinations of these regions. The combination $D = AGF/E^2$ is used because it yields the smallest statistical uncertainty. Similar to the tracker-only analysis, events in the G region are reweighted to match the η distribution in the B region. From a consideration of the observed spread in background estimates from the other combinations, a 20% systematic uncertainty is assigned to the background estimate. The 20% systematic uncertainty is also assigned to the background estimate for the tracker-only analysis.

In order to check the background prediction, loose selection samples, which would be dominated by background tracks, are used for the tracker-only and tracker+TOF analyses. The loose
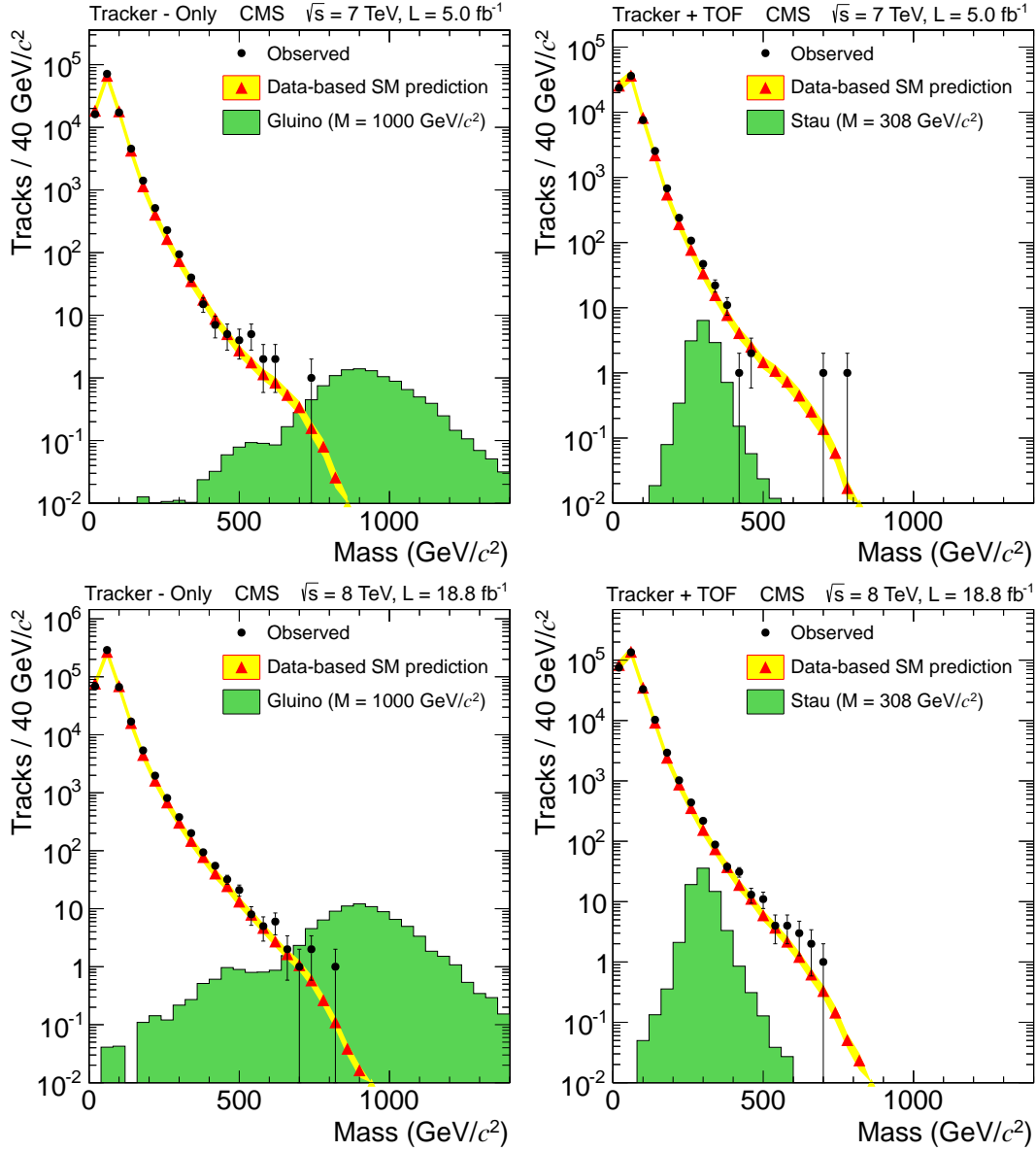
Figure 3: Observed and predicted mass spectra for candidates entering the tracker-only (left column) or tracker+TOF (right column) signal region for the loose selection. The expected distribution for a representative signal scaled to the integrated luminosity is shown as the shaded histogram. The top (bottom) row is for $\sqrt{s} = 7$ (8) TeV.

selection sample for the tracker-only analysis is defined as $p_T > 50\,\text{GeV}/c$ and $I_{as} > 0.10$. The loose selection sample for the tracker+TOF analysis is defined as $p_T > 50\,\text{GeV}/c$, $I_{as} > 0.05$, and $1/\beta > 1.05$. Figure 3 shows the observed and predicted mass spectra for these samples.

The muon-only analysis uses the p_T and $1/\beta$ criteria for the *ABCD* method. The final selections are $p_T > 230\,\text{GeV}/c$ and $1/\beta > 1.4$. It has been found that these variables are correlated with $|\eta|$ and with the number of muon stations used to fit the candidate. Therefore, the background prediction is performed in six separate bins (2/3/4 muon stations in central ($|\eta| < 0.9$) and forward ($0.9 < |\eta| < 2.1$) regions). The final result is computed from a sum of these six bins. The systematic uncertainty in this background estimate is determined by defining four additional regions A', B', C', and D'. Events in B' (A') pass (fail) the p_T requirement, but with
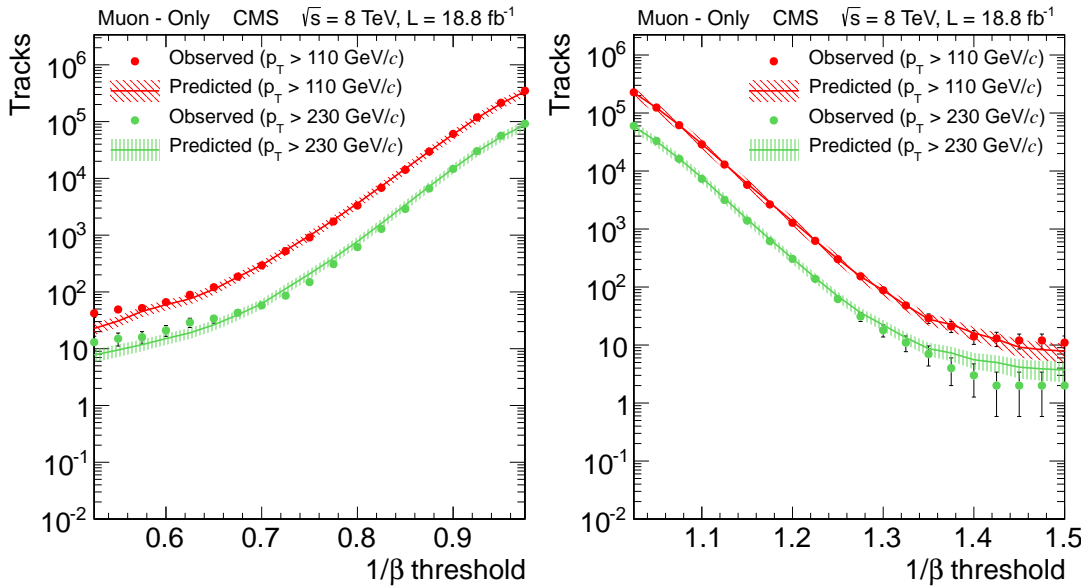
Figure 4: Observed and predicted numbers of tracks in both the control region with $1/\beta < 1$ (left) and the signal region (right) as functions of the $1/\beta$ threshold and for two different p_T thresholds for the muon-only analysis at $\sqrt{s} = 8\,\text{TeV}$. Only statistical uncertainties are shown.

$0.8 < 1/\beta < 1.0$, while events in D' (C') pass (fail) the p_T requirement with $1/\beta < 0.8$. Two complementary predictions now become possible, $D = CB'/A'$ and $D = CD'/C'$. From a consideration of the spread of the three estimates, a systematic uncertainty of 20% is assigned to the background estimate for the muon-only analysis using this method.

The muon-only analysis also has background contributions from cosmic ray muons even after the previously mentioned cosmic ray muon veto requirements are applied. The number of cosmic ray muons expected to pass the selection criteria is determined by using the sideband region of $70 < |d_z| < 120\,\text{cm}$. To increase the number of cosmic ray muons in the sideband region, the veto requirements are not applied here. To reduce the contamination in the sideband region due to muons from collisions, the tracks are required to not be reconstructed in the inner tracker. The number of tracks (N) in the sideband with $1/\beta$ greater than the threshold is counted. To determine the ratio (R_μ) of candidates in the signal region with respect to the sideband region, a pure cosmic ray sample is used. The sample is collected using a trigger requiring a track from the muon system with $p_T > 20\,\text{GeV}/c$, rejecting events within $\pm 50\,\text{ns}$ of a beam crossing and events triggered as beam halo. The cosmic ray muon contribution to the muon-only analysis signal region is determined as $N \times R_\mu$. A similar procedure is used to subtract the estimated cosmic ray muon contribution to the A, B, and C regions prior to estimating the collision muon background in the D region. The cosmic ray muon contribution to the signal region constitutes approximately 60% of the total expected background. The systematic uncertainty in the cosmic ray muon contribution is determined by comparing estimates using $|d_z|$ ranges of 30–50 cm, 50–70 cm, 70–120 cm, and >120 cm. It is found to be 80%. Figure 4 shows the numbers of predicted and observed candidates in both the control region with $1/\beta < 1$ and the signal region for various p_T and $1/\beta$ thresholds for the $\sqrt{s} = 8\,\text{TeV}$ data. The number of predicted events includes both the cosmic ray muon and collision muon contributions. Only statistical uncertainties are shown.

The multiply charged analysis uses the I_{as} and $1/\beta$ criteria. Since the default track reconstruction code assumes $|Q| = 1e$ for p_T determination, the transverse momentum for $|Q| > 1e$
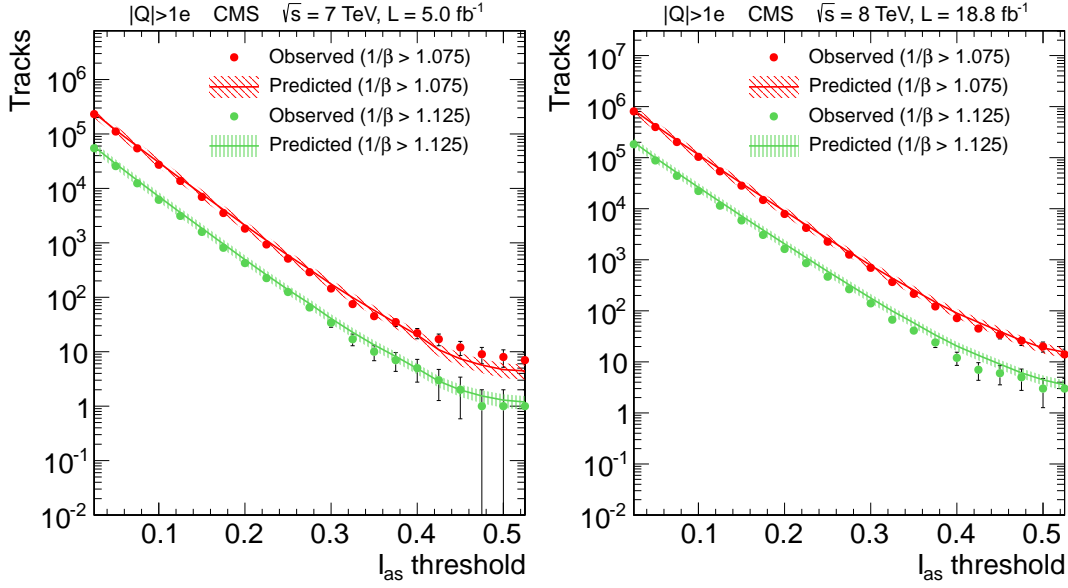
Figure 5: Observed and predicted numbers of tracks as a function of the I_{as} threshold for two different $1/\beta$ thresholds at $\sqrt{s} = 7\,\text{TeV}$ (left) and $8\,\text{TeV}$ (right) for the multiply charged analysis. Only statistical uncertainties are shown.

particles is underestimated by a factor of $1e/|Q|$. Therefore p_T is not used in the final selection. In addition, while dE/dx scales as Q^2, the dynamic range of the silicon readout of individual strips saturates for energy losses ≈ 3 times that of a $\beta \approx 1$, $|Q| = 1e$ particle. Since both the p_T scaling and the dE/dx saturation effects can bias the reconstructed mass to lower values (less separation from background), the reconstructed mass is not used for this analysis. Despite the saturation effect, $|Q| > 1e$ particles have a larger incompatibility of their dE/dx measurements with the MIP hypothesis, increasing the separation power of the dE/dx discriminator for multiply charged particles, relative to that for $|Q| = 1e$ HSCPs. The systematic uncertainty in the background estimate for the multiply charged analysis is determined by the same method that is used for the collision muon background in the muon-only analysis except with p_T changed to be I_{as}. The two complementary estimates from the $1/\beta < 1.0$ region lead to a 20% uncertainty. Figure 5 shows the numbers of predicted and observed candidates for various I_{as} and $1/\beta$ thresholds. Only the statistical uncertainties are shown.

The fractionally charged analysis uses the same method to estimate the background as the tracker-only analysis, replacing the I_{as} variable with I'_{as} and not applying a mass requirement. The systematic uncertainty in the prediction is taken from the tracker+TOF analysis. In addition, the cosmic ray muon background is studied, since particles passing through the tracker not synchronized with the LHC clock often produce tracker hits with low energy readout. The cosmic ray muon background is found to be small and a 50% uncertainty is assigned to this prediction. The numbers of predicted and observed candidates for various p_T and I_{as} thresholds can be seen in Fig. 6. Only the statistical uncertainties are shown.

For each analysis, fixed selections on the appropriate set of I_{as}, I'_{as}, p_T, and $1/\beta$ are used to define the final signal region (and the regions for the background prediction). These values are chosen to give discovery potential over the signal mass regions of interest. For the tracker-only and tracker+TOF analyses, an additional requirement on the reconstructed mass is applied. The mass requirement depends upon the HSCP signal. For a given model and HSCP mass, the range is $M_\text{reco} - 2\sigma$ to $2\,\text{TeV}/c^2$ where M_reco is the average reconstructed mass for the given
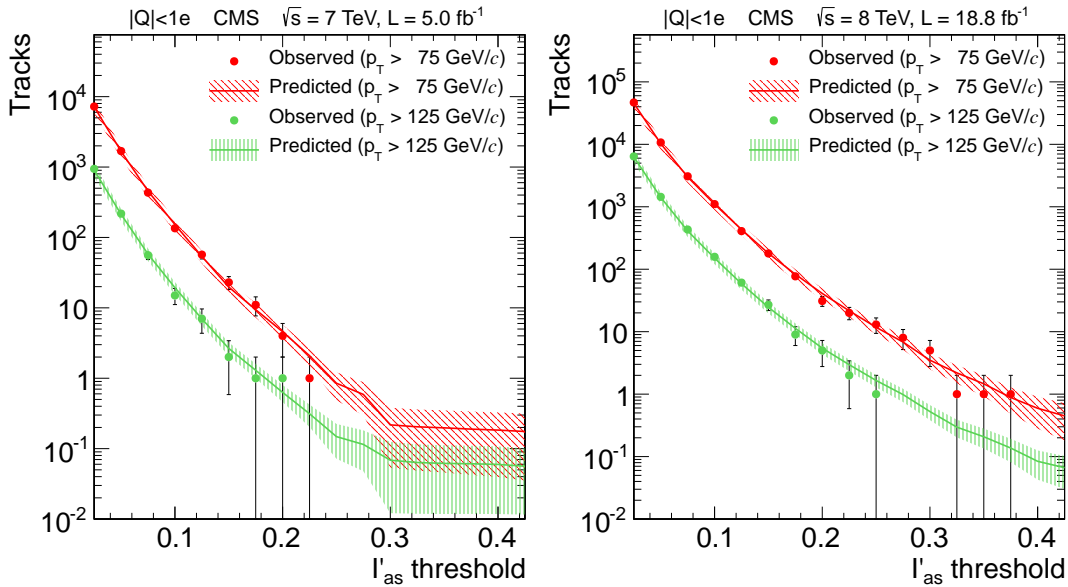
Figure 6: Observed and predicted numbers of tracks as a function of the I'_{as} threshold for two different p_T thresholds at $\sqrt{s} = 7$ TeV (left) and 8 TeV (right) for the fractionally charged analysis. Only statistical uncertainties are shown.

HSCP mass and σ is the expected resolution. Both M_{reco} and σ are determined from simulation.

Table 3 lists the final selection criteria, the predicted numbers of background events, and the numbers of events observed in the signal region. Agreement between prediction and observation is seen over the full range of analyses. Figure 7 shows the observed and predicted mass distributions for the tracker-only and tracker+TOF analyses with the tight selection. The bump at lower mass values expected from the signal MC is due to the saturation of the strip electronic readout.

6 Systematic uncertainties

The sources of systematic uncertainty include those related to the integrated luminosity, the background prediction, and the signal acceptance. The uncertainty in the integrated luminosity is 2.2% (4.4%) at $\sqrt{s} = 7$ (8) TeV [59, 60]. The uncertainties in the background predictions are described in Section 5.

The signal acceptance is obtained from MC simulations of the various signals processed through the full detector simulation (Section 2). Systematic uncertainties in the final results are dominated by uncertainties in the differences between the simulation and data evaluated in control samples. The relevant differences are discussed below. A summary of the systematic uncertainties is given in Table 4.

The trigger acceptance is dominated by the muon triggers for all the models except for the charge-suppressed scenarios. The uncertainty in the muon trigger acceptance arises from several effects. A difference of up to 5% between data and MC simulation events has been observed [58]. For slow moving particles, the effect of the timing synchronization of the muon system is tested by shifting the arrival times in simulation to match the synchronization offset and width observed in data, resulting in an acceptance change of 2% (4%) for $\sqrt{s} = 7$ (8) TeV. For the $|Q| < 1e$ samples, an additional uncertainty arises from the possibility of losing hits
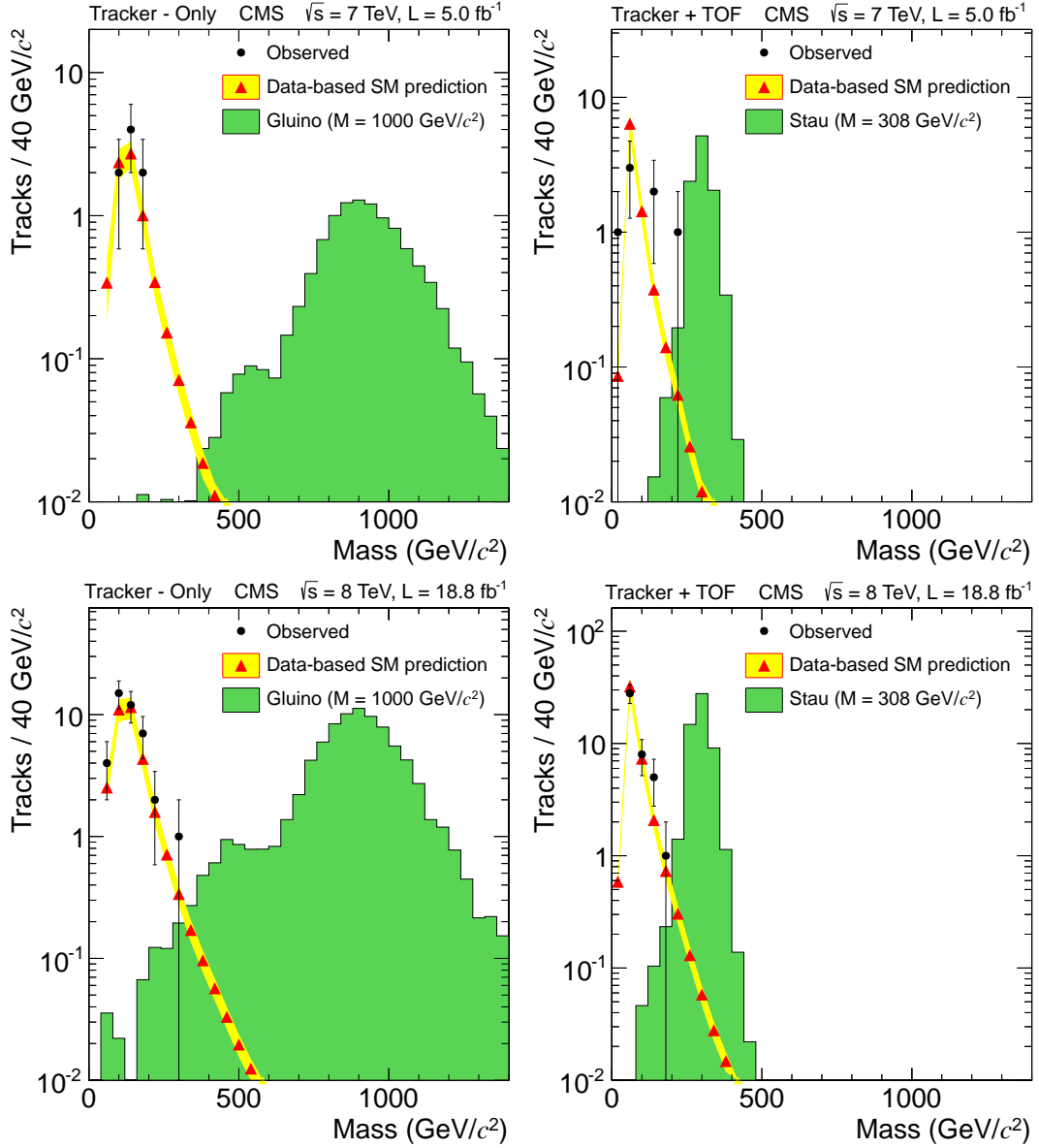
Figure 7: Observed and predicted mass spectra for candidates entering the tracker-only (left column) or tracker+TOF (right column) signal region for the tight selection. The expected distribution for a representative signal scaled to the integrated luminosity is shown as the shaded histogram. The top (bottom) row is for $\sqrt{s} = 7$ (8) TeV.

Table 3: Results of the final selections for the predicted background and the observed numbers of events. The uncertainties include both statistical and systematic contributions.

		Selection criteria			Number of events $\sqrt{s} = 7\,\text{TeV}$		$\sqrt{s} = 8\,\text{TeV}$	
	p_T (GeV/c)	$I_{as}^{(\prime)}$	$1/\beta$	Mass (GeV/c^2)	Pred.	Obs.	Pred.	Obs.
Tracker-only	>70	>0.4	—	>0	7.1 ± 1.5	8	33 ± 7	41
				>100	6.0 ± 1.3	7	26 ± 5	29
				>200	0.65 ± 0.14	0	3.1 ± 0.6	3
				>300	0.11 ± 0.02	0	0.55 ± 0.11	1
				>400	0.030 ± 0.006	0	0.15 ± 0.03	0
Tracker+TOF	>70	>0.125	>1.225	>0	8.5 ± 1.7	7	44 ± 9	42
				>100	1.0 ± 0.2	3	5.6 ± 1.1	7
				>200	0.11 ± 0.02	1	0.56 ± 0.11	0
				>300	0.020 ± 0.004	0	0.090 ± 0.02	0
Muon-only	>230	—	>1.40	—	—	—	6 ± 3	3
$|Q| > 1e$	—	>0.500	>1.200	—	0.15 ± 0.04	0	0.52 ± 0.11	1
$|Q| < 1e$	>125	>0.275	—	—	0.12 ± 0.07	0	1.0 ± 0.2	0

because their ionization in the muon system is closer to the hit threshold. The uncertainty in the gains in the muon system is evaluated by shifting the gain by 25%, yielding an acceptance change of 15% (3%) for $|Q| = e/3(2e/3)$ samples. The uncertainty in the E_T^miss trigger acceptance is found by varying, at HLT level, the energy of simulated jets by the scale uncertainties. The E_T^miss uncertainty for $\sqrt{s} = 7\,\text{TeV}$ samples is estimated to be less than 2% for all scenarios except for the charge-suppressed ones, where it is estimated to be <5%. For $\sqrt{s} = 8\,\text{TeV}$ samples it is less than 1% for all samples.

The energy loss in the silicon tracker is important for all the analyses except for the muon-only one. Low-momentum protons are used to quantify the agreement between the observed and simulated distributions for I_h and I_{as}. The dE/dx distributions of signal samples are varied in the simulation by the observed differences, in order to determine the systematic uncertainty. Because the fractionally charged analysis is also sensitive to changes to the number of hits on the track, track reconstruction is also performed after shifting dE/dx. The uncertainty in the signal acceptance varies by less than 24% for the $|Q| = 1e$ samples, being less than 10% for all masses above 200 GeV/c^2. For the $|Q| < 1e$ samples, the effect of the dE/dx shift and the track reconstruction combined is 25% (<10%) for $|Q| = e/3(2e/3)$. The $|Q| > 1e$ samples have sufficient separation of the signal from the final I_{as} selection that the effect of the dE/dx shift is negligible.

The Z boson decays to muons are used to test the MC simulation of the $1/\beta$ measurement. At $\sqrt{s} = 7\,\text{TeV}$, the $1/\beta$ measurement was observed to have a disagreement of 0.02 in the CSC system and 0.003 in the DT system. At $\sqrt{s} = 8\,\text{TeV}$ a disagreement of 0.005 is observed for both systems. The uncertainty in the signal acceptance is estimated to be between 0 and 15% by shifting $1/\beta$ by these amounts. The uncertainty is generally less than 7% except for the high-charge/low-mass samples in the multiply charged analysis.

The uncertainties in the efficiencies for muon reconstruction [58] and track reconstruction [61] are less than 2% each. The track momentum uncertainty for the muon-only analysis is determined by shifting $1/p_\text{T}$ of muon system tracks by 10%. For all other analyses, the momentum from the inner tracker track is varied as in Ref. [24]. The uncertainty is estimated to be <5% for all but the $|Q| < 1e$ samples, low-mass $|Q| > 1e$ samples, and the muon-only scenarios, where

Table 4: Systematic uncertainties for the various HSCP searches.

Signal acceptance	$|Q| < 1e$	Tracker-only	Tracker+TOF	$|Q| > 1e$	Muon-only
— Trigger acceptance	<16%	<7%	<7%	<6%	7%
— Track momentum scale	< 10%	<4%	< 3%	<10%	<10%
— Track reconstruction eff.	<25%	<2%	<2%	<2%	–
— Ionization energy loss		<18%	<15%	<12%	–
— Time-of-flight	–	–	<2%	<15%	<3%
— Muon reconstruction eff.	–	–	2%	2%	2%
— Pile-up	<2%	<2%	<2%	<2%	<4%
— Detector material	<1%	<1%	<1%	20%	<1%
Total signal acceptance	<31%	<32%	<31%	<29%	<13%
Expected collision bckg.	20%	20%	20%	20%	20%
Expected cosmic ray bckg.	50%	–	–	–	80%
Integrated luminosity	2.2% (4.4%) for $\sqrt{s} = 7$ (8) TeV

the uncertainty is less than 10%.

The uncertainty in the number of pileup events is evaluated by varying by 5-6% the minimum bias cross section used to calculate the weights applied to signal events in order to reproduce the pileup observed in data. This results in uncertainties due to pileup of less than 4%.

The uncertainty in the amount of material in the detector simulation results in an uncertainty in the signal trigger and reconstruction acceptance, particularly for the $|Q| > 1e$ samples. This is evaluated by increasing the amount of material in the hadronic calorimeter by a conservative 5% [62]. Since it was not practical to evaluate the effect in detail for each value of Q considered, the largest change in signal acceptance observed ($\sim$20%) was assigned to all $|Q| > 1e$ scenarios. The change in signal acceptance is ≤ 1% for all $|Q| \leq 1e$ scenarios.

The total systematic uncertainty in the signal acceptance for the tracker-only analysis is less than 32% and is less than 11% for all of the gluino and scalar top cases. For the tracker+TOF analysis it is less than 15% for all cases except for $|Q| = 2e/3$, where the uncertainty ranges from 15% to 31%, being larger at low masses. The muon-only analysis has an uncertainty in the signal acceptance in the range of 7–13%. The multiply charged analysis has an uncertainty in the signal acceptance in the range of 21–29% for $|Q| > 1e$ samples and 7–13% for $|Q| = 1e$ samples with both being larger at low masses. The fractionally charged analysis has an uncertainty in the signal acceptance of 31% and 12% for $|Q| = e/3$ and $2e/3$ samples, respectively.

The statistical uncertainty in the signal acceptance is small compared to the total systematic uncertainty for all the cases except for the low-mass highly charged scenarios, where the low acceptance leads to a statistical uncertainty that is comparable with the systematic uncertainties. For example, in the $|Q| = 6e$, $M = 100\,\text{GeV}/c^2$ signal, the statistical uncertainty is as high as 30%. In all cases the statistical uncertainty is taken into account when setting limits on signal cross sections.

7 Results

No significant excess of events is observed over the predicted backgrounds. The largest excess for any of the selections shown in Table 3 has a significance of 1.3 standard deviations. Cross

section limits are placed at 95% confidence level (CL) for both $\sqrt{s} = 7$ and $8\,\text{TeV}$ using the CL_s approach [63, 64] where p-values are computed with a hybrid bayesian-frequentist technique [65] that uses a lognormal model [54, 55] for the nuisance parameters. The latter are the integrated luminosity, the signal acceptance, and the expected background in the signal region. The uncertainty in the theoretical cross section is not considered as a nuisance parameter. For the combined dataset, the limits are instead placed on the signal strength ($\mu = \sigma/\sigma_{\text{th}}$). Limits on the signal strength using only the $8\,\text{TeV}$ dataset for the muon-only analysis are also presented. The observed limits are shown in Figs. 8–10 for all the analyses along with the theoretical predictions. For the gluino and scalar top pair production, the theoretical cross sections are computed at NLO+NLL [45–48] using PROSPINO [66] with CTEQ6.6M PDFs [67]. The uncertainty bands on the theoretical cross sections include the PDF uncertainty, as well as the α_s and scale uncertainties. Mass limits are obtained from the intersection of the observed limit and the central value of the theoretical cross section. For the combined result, the masses for which the signal strength is less than one are excluded.

From the final results, 95% CL limits on the production cross section are shown in Tables 5, 6, 7, and 8 for gluino, scalar top, stau, and for Drell–Yan like production of fractionally, singly, or multiply charged particles, respectively. The limits are determined from the numbers of events passing all final criteria (including the mass criteria for the tracker-only and tracker+TOF analyses). Figure 8 shows the limits as a function of mass for the tracker-only and tracker+TOF analyses. The tracker-only analysis excludes gluino masses below 1322 and $1233\,\text{GeV}/c^2$ for $f = 0.1$ in the cloud interaction model and charge-suppressed model, respectively. Stop masses below 935 (818) GeV/c^2 are excluded for the cloud (charge-suppressed) models. In addition, the tracker+TOF analysis excludes $\widetilde{\tau}_1$ masses below 500 (339) GeV/c^2 for the direct+indirect (direct only) production. Drell–Yan signals with $|Q| = 2e/3$ and $|Q| = 1e$ are excluded below 220 and $574\,\text{GeV}/c^2$, respectively.

The limits from the muon-only analysis for the scalar top and the gluino with various hadronization fractions f are shown in Fig. 9. The muon-only analysis excludes gluino masses below $1250(1276)\,\text{GeV}/c^2$ for $f = 1.0(0.5)$.

Figure 10 shows the limits applied to the Drell–Yan production model for both the fractionally charged and multiply charged analyses. The fractionally charged analysis excludes masses below 200 and $480\,\text{GeV}/c^2$ for $|Q| = e/3$ and $2e/3$, respectively. The multiply charged analysis excludes masses below 685, 752, 793, 796, 781, 757, and $715\,\text{GeV}/c^2$ for $|Q| = 2e$, $3e$, $4e$, $5e$, $6e$, $7e$, and $8e$, respectively. The multiply charged analysis is not optimized for singly charged particles but can set a limit and is able to exclude masses below $517\,\text{GeV}/c^2$. As expected, this limit is not as stringent as the one set by the tracker+TOF analysis but does allow results to be interpolated to non-integer charge values (such as $|Q| = 3e/2$, $4e/3$) using results from the same analysis.

The mass limits for various signals and electric charges are shown in Fig. 11 and are compared with previously published results.

The limits obtained for the reanalyzed $\sqrt{s} = 7\,\text{TeV}$ dataset are similar to the previously published CMS results except for the stau scenarios, where the new cross section limits are slightly worse than the previously published ones. This result is a consequence of having a common selection for all mass points and models in contrast to what was done in Ref. [24], where the selection was optimized separately for each mass point and model. However, the use of a higher NLO cross section for the indirect production of staus than in Ref. [24] results in more stringent limits on the stau mass.
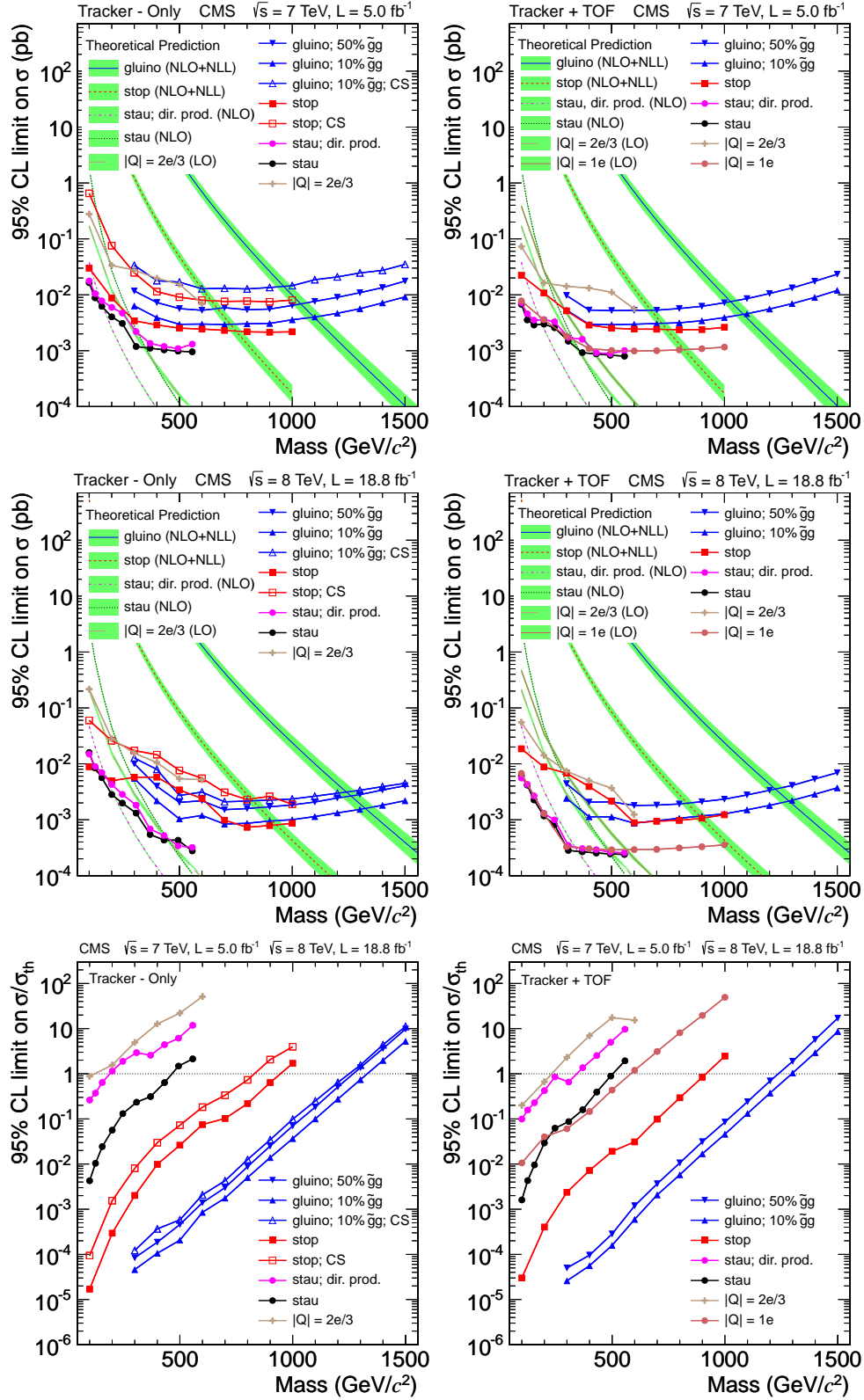
Figure 8: Upper cross section limits at 95% CL on various signal models for the tracker-only analysis (left column) and tracker+TOF analysis (right column). The top row is for the data at $\sqrt{s} = 7\,\text{TeV}$, the middle row is for the data at $\sqrt{s} = 8\,\text{TeV}$, the bottom row shows the ratio of the limit to the theoretical value for the combined dataset. In the legend, 'CS' stands for the charge-suppressed interaction model.
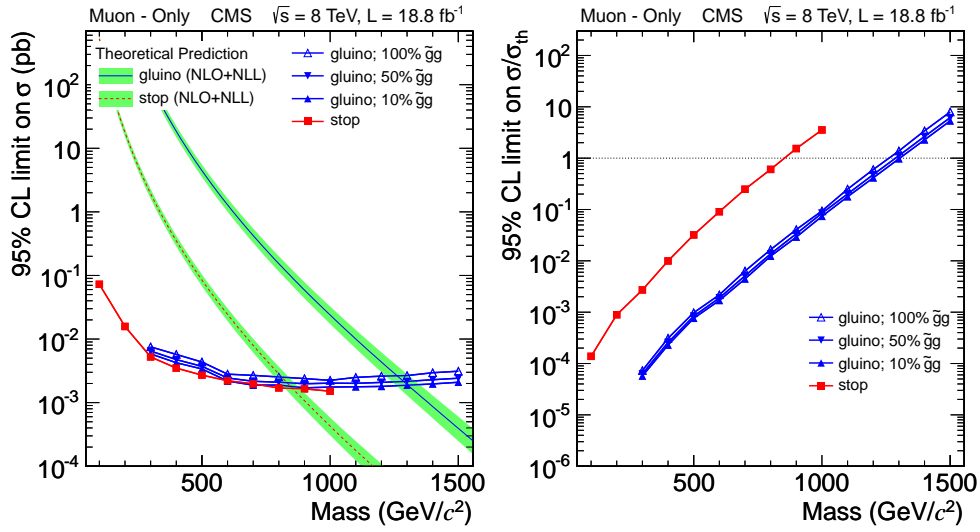
Figure 9: Upper cross section limits at 95% CL on various signal models for the muon-only analysis for the data at $\sqrt{s} = 8\,\text{TeV}$ (left). Limits on the signal strength ($\mu = \sigma/\sigma_\text{th}$) for the same data (right).

Table 5: Expected and observed cross section limits and the signal acceptance for gluino signals at $\sqrt{s} = 7$ and $8\,\text{TeV}$, as well as the ratio of the cross section limit to the theoretical value for the combined dataset. The limit on the ratio for the muon-only analysis uses only $\sqrt{s} = 8\,\text{TeV}$ data. The minimum reconstructed mass required (M req.) for each sample in the tracker-only analysis is also given.

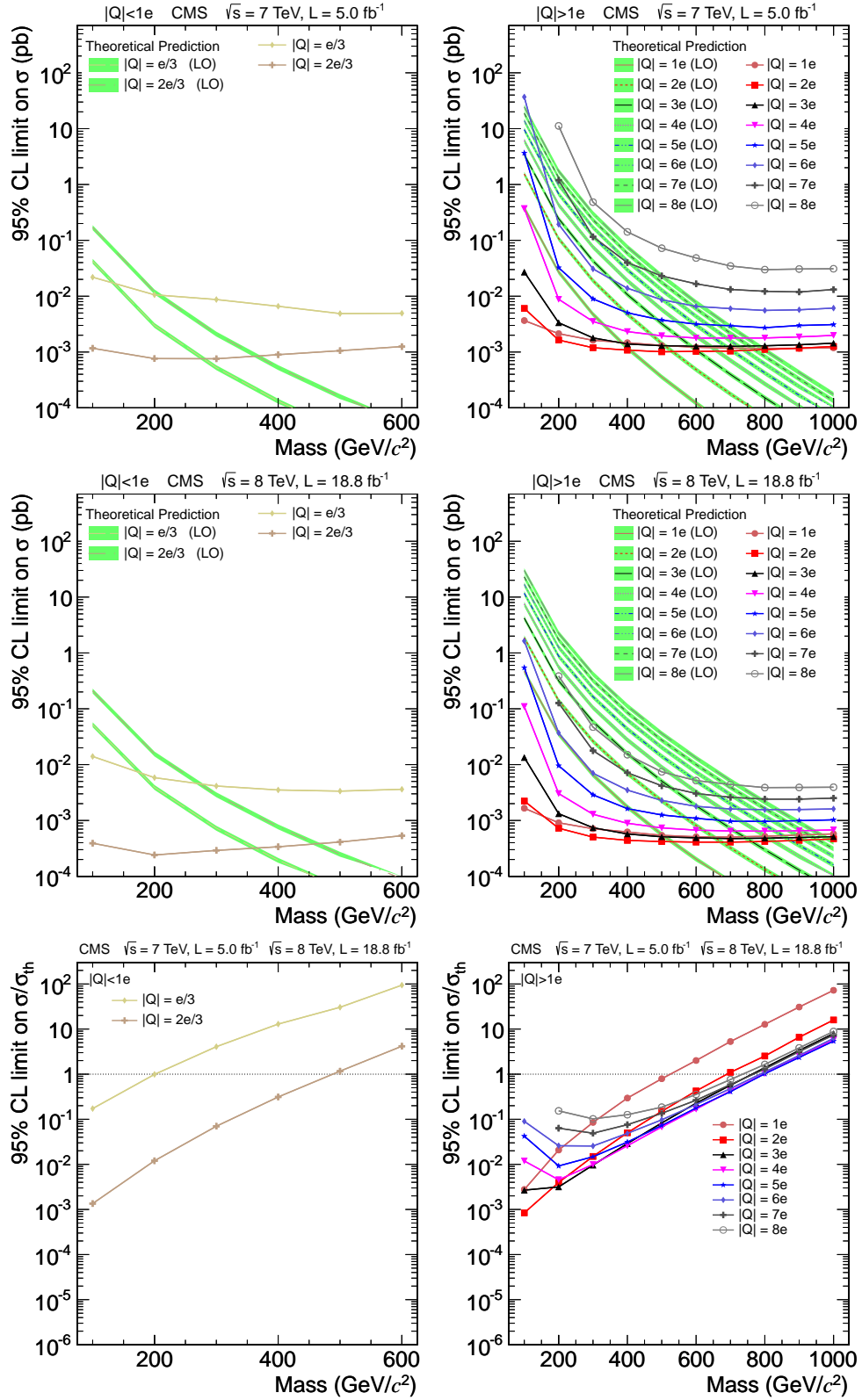| Mass (GeV/c^2)	M req. (GeV/c^2)	σ (pb) ($\sqrt{s} = 7\,\text{TeV}$)			σ (pb) ($\sqrt{s} = 8\,\text{TeV}$)			σ/σ_th (7+8 TeV)	
		Exp.	Obs.	Acc.	Exp.	Obs.	Acc.	Exp.	Obs.
Gluino ($f = 0.1$) — tracker-only analysis									
300	>100	0.0046	0.0063	0.17	0.0055	0.0055	0.15	4.0×10^{-5}	4.6×10^{-5}
700	>370	0.0028	0.0029	0.21	0.00081	0.00084	0.19	0.0017	0.0018
1100	>540	0.0039	0.0040	0.15	0.0010	0.0011	0.14	0.098	0.10
1500	>530	0.0088	0.0092	0.066	0.0021	0.0022	0.073	5.1	5.2
Gluino charge-suppressed ($f = 0.1$) — tracker-only analysis									
300	>130	0.035	0.034	0.021	0.013	0.013	0.048	0.00011	0.00012
700	>340	0.012	0.013	0.046	0.0020	0.0021	0.077	0.0044	0.0043
1100	>410	0.018	0.019	0.033	0.0025	0.0026	0.061	0.24	0.25
1500	>340	0.034	0.035	0.017	0.0045	0.0045	0.035	11	11
Gluino ($f = 0.5$) — muon-only analysis									
300	–	–	–	–	0.0060	0.0065	0.058	5.8×10^{-5}	6.3×10^{-5}
700	–	–	–	–	0.0026	0.0022	0.12	0.0062	0.0051
1100	–	–	–	–	0.0024	0.0020	0.13	0.24	0.20
1500	–	–	–	–	0.0030	0.0024	0.11	7.5	6.2
Gluino ($f = 1.0$) — muon-only analysis									
300	–	–	–	–	0.0070	0.0075	0.050	6.8×10^{-5}	7.3×10^{-5}
700	–	–	–	–	0.0032	0.0027	0.10	0.0075	0.0063
1100	–	–	–	–	0.0030	0.0025	0.11	0.30	0.25
1500	–	–	–	–	0.0037	0.0031	0.087	9.5	7.9

Figure 10: Upper cross section limits at 95% CL on various signal models for the fractionally charged analysis (left column) and multiply charged analysis (right column). The top row is for the data at $\sqrt{s} = 7\,\mathrm{TeV}$, the middle row is for the data at $\sqrt{s} = 8\,\mathrm{TeV}$, the bottom row shows the ratio of the limit to the theoretical value for the combined dataset.

Table 6: Expected and observed cross section limits and the signal acceptance for scalar top signals at $\sqrt{s} = 7$ and 8 TeV, as well as the ratio of the cross section limit to the theoretical value for the combined dataset. The minimum reconstructed mass required (M req.) for each sample in the tracker-only analysis is also given.

Mass (GeV/c^2)	M req. (GeV/c^2)	σ (pb) ($\sqrt{s} = 7\,\mathrm{TeV}$)			σ (pb) ($\sqrt{s} = 8\,\mathrm{TeV}$)			$\sigma/\sigma_{\mathrm{th}}$ (7+8 TeV)	
		Exp.	Obs.	Acc.	Exp.	Obs.	Acc.	Exp.	Obs.
		Stop	—	tracker-only analysis					
200	>0	0.0080	0.0088	0.14	0.0051	0.0050	0.18	0.00026	0.00029
500	>120	0.0024	0.0025	0.24	0.0027	0.0034	0.23	0.022	0.026
800	>330	0.0021	0.0022	0.28	0.00072	0.00073	0.22	0.21	0.22
		Stop charge-suppressed	—	tracker-only analysis					
200	>0	0.063	0.075	0.020	0.018	0.026	0.050	0.0011	0.0014
500	>120	0.0086	0.0089	0.066	0.0068	0.0081	0.10	0.062	0.070
800	>270	0.0071	0.0076	0.079	0.0019	0.0023	0.10	0.61	0.74

Table 7: Expected and observed cross section limits and the signal acceptance for stau signals at $\sqrt{s} = 7$ and 8 TeV, as well as the ratio of the cross section limit to the theoretical value for the combined dataset. The minimum reconstructed mass required (M req.) for each sample in the tracker+TOF analysis is also given.

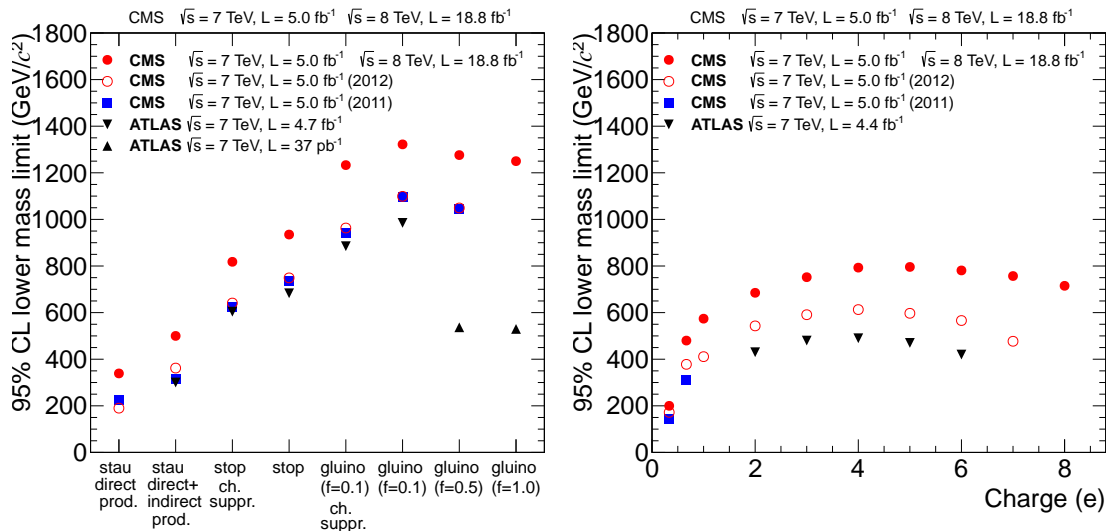| Mass (GeV/c^2)	M req. (GeV/c^2)	σ (pb) ($\sqrt{s} = 7\,\mathrm{TeV}$)			σ (pb) ($\sqrt{s} = 8\,\mathrm{TeV}$)			$\sigma/\sigma_{\mathrm{th}}$ (7+8 TeV)	
		Exp.	Obs.	Acc.	Exp.	Obs.	Acc.	Exp.	Obs.
		Direct+indirect produced stau	—	tracker+TOF analysis					
126	>40	0.0046	0.0035	0.29	0.0042	0.0042	0.25	0.0050	0.0043
308	>190	0.00094	0.0015	0.63	0.00029	0.00028	0.56	0.065	0.087
494	>330	0.00079	0.00084	0.74	0.00023	0.00024	0.66	0.66	0.84
		Direct produced stau	—	tracker+TOF analysis					
126	>40	0.0056	0.0046	0.26	0.0044	0.0043	0.24	0.18	0.16
308	>190	0.0011	0.0017	0.54	0.00035	0.00035	0.46	0.62	0.66
494	>330	0.00084	0.00088	0.69	0.00025	0.00026	0.61	4.7	5.0

Figure 11: Lower mass limits at 95% CL for various models compared with previously published results [19–26]. The model type is given on the x-axis (left). Mass limits are shown for Drell–Yan like production of fractionally, singly, and multiply charged particles (right). These particles were assumed to be neutral under $SU(3)_C$ and $SU(2)_L$.

Table 8: Expected and observed cross section limits and the signal acceptance for the Drell–Yan like production of fractionally, singly, and multiply charged particles at $\sqrt{s} = 7$ and $8\,\text{TeV}$, as well as the ratio of the cross section limit to the theoretical value for the combined dataset. The minimum reconstructed mass required (M req.) for each sample in the tracker+TOF analysis is also given.

Mass (GeV/c^2)	M req. (GeV/c^2)	σ (pb) ($\sqrt{s} = 7\,\text{TeV}$)			σ (pb) ($\sqrt{s} = 8\,\text{TeV}$)			$\sigma/\sigma_{\text{th}}$ (7+8 TeV)	
		Exp.	Obs.	Acc.	Exp.	Obs.	Acc.	Exp.	Obs.
		Drell–Yan like production $|Q| = e/3$ — $|Q| < 1e$ analysis							
100	–	0.019	0.022	0.029	0.016	0.014	0.012	0.19	0.17
200	–	0.0094	0.011	0.060	0.0066	0.0058	0.030	1.2	0.99
400	–	0.0058	0.0066	0.098	0.0041	0.0035	0.048	15	13
		Drell–Yan like production $|Q| = 2e/3$ — $|Q| < 1e$ analysis							
100	–	0.0011	0.0012	0.53	0.00042	0.00039	0.45	0.0015	0.0013
200	–	0.00071	0.00076	0.81	0.00027	0.00024	0.68	0.014	0.012
400	–	0.00083	0.00090	0.68	0.00033	0.00034	0.56	0.35	0.31
		Drell–Yan like production $|Q| = 1e$ — tracker+TOF analysis							
200	>120	0.0015	0.0036	0.41	0.00077	0.0013	0.36	0.019	0.040
500	>340	0.00098	0.0010	0.60	0.00028	0.00029	0.56	0.41	0.44
800	>530	0.0010	0.0010	0.58	0.00030	0.00031	0.52	7.5	8.1
		Drell–Yan like production $|Q| = 2e$ — $|Q| > 1e$ analysis							
200	–	0.0016	0.0016	0.36	0.00050	0.00073	0.33	0.0028	0.0040
500	–	0.00098	0.0010	0.59	0.00029	0.00042	0.56	0.11	0.15
800	–	0.0011	0.0011	0.55	0.00029	0.00042	0.56	1.9	2.5
		Drell–Yan like production $|Q| = 3e$ — $|Q| > 1e$ analysis							
200	–	0.0031	0.0034	0.18	0.00090	0.0013	0.18	0.0023	0.0032
500	–	0.0012	0.0013	0.47	0.00035	0.00051	0.46	0.059	0.083
800	–	0.0012	0.0013	0.47	0.00033	0.00048	0.49	0.99	1.4
		Drell–Yan like production $|Q| = 4e$ — $|Q| > 1e$ analysis							
200	–	0.0082	0.0088	0.069	0.0021	0.0030	0.078	0.0031	0.0045
500	–	0.0018	0.0020	0.31	0.00051	0.00074	0.32	0.048	0.068
800	–	0.0017	0.0018	0.34	0.00045	0.00064	0.37	0.75	1.0
		Drell–Yan like production $|Q| = 5e$ — $|Q| > 1e$ analysis							
200	–	0.030	0.032	0.019	0.0066	0.0096	0.025	0.0064	0.0092
500	–	0.0035	0.0037	0.16	0.00086	0.0013	0.19	0.052	0.073
800	–	0.0026	0.0027	0.22	0.00066	0.00096	0.24	0.71	1.0
		Drell–Yan like production $|Q| = 6e$ — $|Q| > 1e$ analysis							
200	–	0.17	0.19	0.0032	0.026	0.037	0.0064	0.018	0.026
500	–	0.0079	0.0086	0.072	0.0016	0.0023	0.10	0.055	0.077
800	–	0.0054	0.0056	0.11	0.0011	0.0016	0.15	0.81	1.1
		Drell–Yan like production $|Q| = 7e$ — $|Q| > 1e$ analysis							
200	–	1.1	1.2	0.00053	0.086	0.13	0.0019	0.047	0.063
500	–	0.022	0.023	0.026	0.0028	0.0042	0.057	0.079	0.11
800	–	0.012	0.012	0.049	0.0017	0.0024	0.099	0.96	1.3
		Drell–Yan like production $|Q| = 8e$ — $|Q| > 1e$ analysis							
200	–	9.8	11	7.1×10^{-5}	0.26	0.38	0.00064	0.11	0.15
500	–	0.068	0.072	0.0084	0.0051	0.0074	0.032	0.11	0.16
800	–	0.028	0.030	0.020	0.0027	0.0039	0.062	1.0	1.4

The mass limit for $|Q| < 1e$ samples are significantly improved with respect to Ref. [23], thanks to a different analysis approach and to the use of the I'_{as} likelihood discriminator that maximally exploits all the dE/dx information associated with a track.

8   Summary

A search for heavy stable charged particles has been presented, based on several different signatures, using data recorded at collision energies of 7 and 8 TeV. Five complementary analyses have been performed: a search with only the inner tracker, a search with both the inner tracker and the muon system, a search with only the muon system, a search for low ionizing tracks, and a search for tracks with very large ionization energy loss. No significant excess is observed in any of the analyses. Limits on cross sections are presented for models with the production of gluinos, scalar tops, and staus, and for Drell–Yan like production of fractionally, singly, and multiply charged particles. The models for R-hadron-like HSCPs include a varying fraction of $\widetilde{g}-$gluon production and two different interaction schemes leading to a variety of non-standard experimental signatures. Lower mass limits for these models are given. Gluino masses below 1322 and 1233 GeV/c^2 are excluded for $f = 0.1$ in the cloud interaction model and the charge-suppressed model, respectively. For $f = 0.5$ (1.0), gluino masses below 1276 (1250) GeV/c^2 are excluded. For stop production, masses below 935 (818) GeV/c^2 are excluded for the cloud (charge-suppressed) models. In addition, these analyses exclude $\widetilde{\tau}_1$ masses below 500 (339) GeV/c^2 for the direct+indirect (direct only) production. Drell–Yan like signals with $|Q| = e/3$, $2e/3$, $1e$, $2e$, $3e$, $4e$, $5e$, $6e$, $7e$, and $8e$ are excluded with masses below 200, 480, 574, 685, 752, 793, 796, 781, 757, and 715 GeV/c^2, respectively. These limits are the most stringent to date.

Acknowledgments

References

[1] M. Drees and X. Tata, "Signals for heavy exotics at hadron colliders and supercolliders", *Phys. Lett. B* **252** (1990) 695, `doi:10.1016/0370-2693(90)90508-4`.

[2] M. Fairbairn et al., "Stable massive particles at colliders", *Phys. Rept.* **438** (2007) 1, `doi:10.1016/j.physrep.2006.10.002`, `arXiv:hep-ph/0611040`.

[3] C. W. Bauer et al., "Supermodels for early LHC", *Phys. Lett. B* **690** (2010) 280, `doi:10.1016/j.physletb.2010.05.032`, `arXiv:0909.5213`.

[4] J. S. Schwinger, "Magnetic charge and quantum field theory", *Phys. Rev.* **144** (1966) 1087, `doi:10.1103/PhysRev.144.1087`.

[5] A. Kusenko and M. E. Shaposhnikov, "Supersymmetric Q-balls as dark matter", *Phys. Lett. B* **418** (1998) 46, `doi:10.1016/S0370-2693(97)01375-0`, `arXiv:hep-ph/9709492`.

[6] D. Fargion, M. Khlopov, and C. A. Stephan, "Cold dark matter by heavy double charged leptons?", *Class. Quant. Grav.* **23** (2006) 7305, `doi:10.1088/0264-9381/23/24/008`, `arXiv:astro-ph/0511789`.

[7] B. Koch, M. Bleicher, and H. Stoecker, "Black holes at LHC?", *J. Phys. G* **34** (2007) S535, `doi:10.1088/0954-3899/34/8/S44`, `arXiv:hep-ph/0702187`.

[8] J. Kang, P. Langacker, and B. D. Nelson, "Theory and Phenomenology of Exotic Isosinglet Quarks and Squarks", *Phys. Rev. D* **77** (2008) 035003, `doi:10.1103/PhysRevD.77.035003`, `arXiv:0708.2701`.

[9] Particle Data Group Collaboration, "Review of Particle Physics", *Phys. Rev. D* **86** (2012) 010001, `doi:10.1103/PhysRevD.86.010001`.

[10] ALEPH Collaboration, "Search for pair production of longlived heavy charged particles in e^+e^- annihilation", *Phys. Lett. B* **405** (1997) 379, `doi:10.1016/S0370-2693(97)00715-6`, `arXiv:hep-ex/9706013`.

[11] DELPHI Collaboration, "Search for heavy stable and longlived particles in e^+e^- collisions at $\sqrt{s} = 189$ GeV", *Phys. Lett. B* **478** (2000) 65, `doi:10.1016/S0370-2693(00)00265-3`, `arXiv:hep-ex/0103038`.

[12] L3 Collaboration, "Search for heavy neutral and charged leptons in e^+e^- annihilation at LEP", *Phys. Lett. B* **517** (2001) 75, `doi:10.1016/S0370-2693(01)01005-X`, `arXiv:hep-ex/0107015`.

[13] OPAL Collaboration, "Search for stable and longlived massive charged particles in e^+e^- collisions at $\sqrt{s} = 130$ GeV to 209 GeV", *Phys. Lett. B* **572** (2003) 8, `doi:10.1016/S0370-2693(03)00639-7`, `arXiv:hep-ex/0305031`.

[14] H1 Collaboration, "Measurement of anti-deuteron photoproduction and a search for heavy stable charged particles at HERA", *Eur. Phys. J. C* **36** (2004) 413, `doi:10.1140/epjc/s2004-01894-1`, `arXiv:hep-ex/0403056`.

[15] D0 Collaboration, "Search for long-lived charged massive particles with the D0 detector", *Phys. Rev. Lett.* **102** (2009) 161802, `doi:10.1103/PhysRevLett.102.161802`, `arXiv:0809.4472`.

[16] CDF Collaboration, "Search for long-lived massive charged particles in 1.96 TeV $\bar{p}p$ collisions", *Phys. Rev. Lett.* **103** (2009) 021802, `doi:10.1103/PhysRevLett.103.021802`, `arXiv:0902.1266`.

[17] D0 Collaboration, "A search for charged massive long-lived particles", *Phys. Rev. Lett.* **108** (2012) 121802, `doi:10.1103/PhysRevLett.108.121802`, `arXiv:1110.3302`.

[18] D0 Collaboration, "Search for charged massive long-lived particles at $\sqrt{s}$=1.96 TeV", *Phys. Rev. D* **87** (2013) 052011, `doi:10.1103/PhysRevD.87.052011`, `arXiv:1211.2466`.

[19] CMS Collaboration, "Search for heavy stable charged particles in pp collisions at $\sqrt{s} = 7$ TeV", *JHEP* **03** (2011) 024, `doi:10.1007/JHEP03(2011)024`, `arXiv:1101.1645`.

[20] ATLAS Collaboration, "Search for massive long-lived highly ionising particles with the ATLAS detector at the LHC", *Phys. Lett. B* **698** (2011) 353, `doi:10.1016/j.physletb.2011.03.033`, `arXiv:1102.0459`.

[21] ATLAS Collaboration, "Search for stable hadronising squarks and gluinos with the ATLAS experiment at the LHC", *Phys. Lett. B* **701** (2011) 1, `doi:10.1016/j.physletb.2011.05.010`, `arXiv:1103.1984`.

[22] ATLAS Collaboration, "Search for heavy long-lived charged particles with the ATLAS detector in pp collisions at $\sqrt{s} = 7$ TeV", *Phys. Lett. B* **703** (2011) 428, `doi:10.1016/j.physletb.2011.08.042`, `arXiv:1106.4495`.

[23] CMS Collaboration, "Search for fractionally charged particles in pp collisions at $\sqrt{s} = 7$ TeV", (2012). `arXiv:1210.2311`.

[24] CMS Collaboration, "Search for heavy long-lived charged particles in pp collisions at $\sqrt{s} = 7$ TeV", *Phys. Lett. B* **713** (2012) 408, `doi:10.1016/j.physletb.2012.06.023`, `arXiv:1205.0272`.

[25] ATLAS Collaboration, "Searches for heavy long-lived sleptons and R-Hadrons with the ATLAS detector in pp collisions at $\sqrt{s} = 7$ TeV", *Phys. Lett. B* **720** (2013) 277, `doi:10.1016/j.physletb.2013.02.015`, `arXiv:1211.1597`.

[26] ATLAS Collaboration, "Search for long-lived, multi-charged particles in pp collisions at $\sqrt{s} = 7$ TeV using the ATLAS detector", (2013). `arXiv:1301.5272`.

[27] C. F. Berger, J. S. Gainer, J. L. Hewett, and T. G. Rizzo, "Supersymmetry Without Prejudice", *JHEP* **02** (2009) 023, `doi:10.1088/1126-6708/2009/02/023`, `arXiv:0812.0980`.

[28] M. W. Cahill-Rowley, J. L. Hewett, A. Ismail, and T. G. Rizzo, "More energy, more searches, but the pMSSM lives on", (2012). `arXiv:1211.1981`.

[29] G. R. Farrar and P. Fayet, "Phenomenology of the production, decay, and detection of new hadronic states associated with supersymmetry", *Phys. Lett. B* **76** (1978) 575, `doi:10.1016/0370-2693(78)90858-4`.

[30] A. C. Kraan, "Interactions of heavy stable hadronizing particles", *Eur. Phys. J. C* **37** (2004) 91, `doi:10.1140/epjc/s2004-01997-7`, `arXiv:hep-ex/0404001`.

[31] R. Mackeprang and A. Rizzi, "Interactions of coloured heavy stable particles in matter", *Eur. Phys. J. C* **50** (2007) 353, `doi:10.1140/epjc/s10052-007-0252-4`, `arXiv:hep-ph/0612161`.

[32] R. Mackeprang and D. Milstead, "An updated description of heavy-hadron interactions in GEANT4", *Eur. Phys. J. C* **66** (2010) 493, `doi:10.1140/epjc/s10052-010-1262-1`, `arXiv:0908.1868`.

[33] S. Agostinelli et al., "Geant4–a simulation toolkit", *Nucl. Instrum. Meth. A* **506** (2003) 250, `doi:10.1016/S0168-9002(03)01368-8`.

[34] J. Allison et al., "Geant4 developments and applications", *IEEE Trans. Nucl. Sci.* **53** (2006) 270, `doi:10.1109/TNS.2006.869826`.

[35] G. F. Giudice and R. Rattazzi, "Theories with gauge mediated supersymmetry breaking", *Phys. Rept.* **322** (1999) 419, `doi:10.1016/S0370-1573(99)00042-3`, `arXiv:hep-ph/9801271`.

[36] T. Sjöstrand, S. Mrenna, and P. Z. Skands, "PYTHIA 6.4 physics and manual", *JHEP* **05** (2006) 026, `doi:10.1088/1126-6708/2006/05/026`, `arXiv:hep-ph/0603175`.

[37] B. C. Allanach et al., "The Snowmass points and slopes: Benchmarks for SUSY searches", *Eur. Phys. J. C* **25** (2002) 113, `doi:10.1007/s10052-002-0949-3`, `arXiv:hep-ph/0202233`.

[38] F. E. Paige, S. D. Protopopescu, H. Baer, and X. Tata, "ISAJET 7.69: A Monte Carlo Event Generator for pp, $\bar{p}p$, and e^+e^- Reactions", (2003). `arXiv:hep-ph/0312045`.

[39] W. Beenakker et al., "The production of charginos/neutralinos and sleptons at hadron colliders", *Phys. Rev. Lett.* **83** (1999) 3780, `doi:10.1103/PhysRevLett.83.3780`, `arXiv:hep-ph/9906298`. Erratum at `doi:10.1103/PhysRevLett.100.029901`.

[40] T. Sjöstrand, S. Mrenna, and P. Z. Skands, "A brief introduction to PYTHIA 8.1", *Comput. Phys. Commun.* **178** (2008) 852, `doi:10.1016/j.cpc.2008.01.036`, `arXiv:0710.3820`.

[41] G. F. Giudice and A. Romanino, "Split supersymmetry", *Nucl. Phys. B* **699** (2004) 65, `doi:10.1016/j.nuclphysb.2004.11.048`, `arXiv:hep-ph/0406088`.

[42] N. Arkani-Hamed and S. Dimopoulos, "Supersymmetric unification without low energy supersymmetry and signatures for fine-tuning at the LHC", *JHEP* **06** (2005) 073, `doi:10.1088/1126-6708/2005/06/073`, `arXiv:hep-th/0405159`.

[43] W. Beenakker, R. Höpker, M. Spira, and P. M. Zerwas, "Squark and gluino production at hadron colliders", *Nucl. Phys. B* **492** (1997) 51, `doi:10.1016/S0550-3213(97)80027-2`, `arXiv:hep-ph/9610490`.

[44] W. Beenakker et al., "Stop production at hadron colliders", *Nucl. Phys. B* **515** (1998) 3, `doi:10.1016/S0550-3213(98)00014-5`, `arXiv:hep-ph/9710451`.

[45] A. Kulesza and L. Motyka, "Threshold resummation for squark-antisquark and gluino-pair production at the LHC", *Phys. Rev. Lett.* **102** (2009) 111802, `doi:10.1103/PhysRevLett.102.111802`, `arXiv:0807.2405`.

[46] W. Beenakker et al., "Soft-gluon resummation for squark and gluino hadroproduction", *JHEP* **12** (2009) 041, `doi:10.1088/1126-6708/2009/12/041`, `arXiv:0909.4418`.

[47] A. Kulesza and L. Motyka, "Soft gluon resummation for the production of gluino-gluino and squark-antisquark pairs at the LHC", *Phys. Rev. D* **80** (2009) 095004, `doi:10.1103/PhysRevD.80.095004`, `arXiv:0905.4749`.

[48] W. Beenakker et al., "Supersymmetric top and bottom squark production at hadron colliders", *JHEP* **08** (2010) 098, `doi:10.1007/JHEP08(2010)098`, `arXiv:1006.4771`.

[49] W. Beenakker et al., "Squark and gluino hadroproduction", *Int. J. Mod. Phys. A* **26** (2011) 2637, `doi:10.1142/S0217751X11053560`, `arXiv:1105.1110`.

[50] M. Krämer et al., "Supersymmetry production cross sections in pp collisions at $\sqrt{s} = 7$ TeV", (2012). `arXiv:1206.2892`.

[51] P. Langacker and G. Steigman, "Requiem for an FCHAMP (Fractionally CHArged, Massive Particle) ?", *Phys. Rev. D* **84** (2011) 065040, `doi:10.1103/PhysRevD.84.065040`, `arXiv:1107.3131`.

[52] J. Pumplin et al., "New generation of parton distributions with uncertainties from global QCD analysis", *JHEP* **07** (2002) 012, `doi:10.1088/1126-6708/2002/07/012`, `arXiv:hep-ph/0201195`.

[53] CMS Collaboration, "The CMS experiment at the CERN LHC", *JINST* **3** (2008) S08004, `doi:10.1088/1748-0221/3/08/S08004`.

[54] W. T. Eadie et al., "Statistical methods in experimental physics". North Holland, Amsterdam, 1971.

[55] F. James, "Statistical methods in experimental physics". World Scientific, Singapore, 2006.

[56] CMS Collaboration, "Determination of Jet Energy Calibration and Transverse Momentum Resolution in CMS", *JINST* **6** (2011) P11002, `doi:10.1088/1748-0221/6/11/P11002`, `arXiv:1107.4277`.

[57] CMS Collaboration, "Particle–flow event reconstruction in CMS and performance for jets, taus, and E_T^{miss}", CMS Physics Analysis Summary CMS-PAS-PFT-09-001, (2009).

[58] CMS Collaboration, "Performance of CMS muon reconstruction in pp collision events at $\sqrt{s} = 7$ TeV", *JINST* **7** (2012) P10002, `doi:10.1088/1748-0221/7/10/P10002`, `arXiv:1206.4071`.

[59] CMS Collaboration, "Absolute Calibration of the Luminosity Measurement at CMS: Winter 2012 Update", CMS Physics Analysis Summary CMS-PAS-SMP-12-008, (2012).

[60] CMS Collaboration, "CMS Luminosity Based on Pixel Cluster Counting - Summer 2012 Update", CMS Physics Analysis Summary CMS-PAS-LUM-12-001, (2012).

[61] CMS Collaboration, "Measurement of tracking efficiency", CMS Physics Analysis Summary CMS-PAS-TRK-10-002, (2010).

[62] CMS Collaboration, "Precise Mapping of the Magnetic Field in the CMS Barrel Yoke using Cosmic Rays", *JINST* **5** (2010) T03021, `doi:10.1088/1748-0221/5/03/T03021`, `arXiv:0910.5530`.

[63] T. Junk, "Confidence level computation for combining searches with small statistics", *Nucl. Instrum. Meth. A* **434** (1999) 435, `doi:10.1016/S0168-9002(99)00498-2`, `arXiv:hep-ex/9902006`.

[64] A. L. Read, "Presentation of search results: the CL_s technique", *J. Phys. G* **28** (2002) 2693, `doi:10.1088/0954-3899/28/10/313`.

[65] ATLAS and CMS Collaborations, "Procedure for the LHC Higgs boson search combination in Summer 2011", Technical Report CMS-NOTE-2011-005, ATL-PHYS-PUB-2011-011, CERN, Geneva, (2011).

[66] W. Beenakker, R. Hopker, and M. Spira, "PROSPINO: A program for the PROduction of Supersymmetric Particles In Next-to-leading Order QCD", (1996). `arXiv:hep-ph/9611232`.

[67] P. M. Nadolsky et al., "Implications of CTEQ global analysis for collider observables", *Phys. Rev. D* **78** (2008) 013004, `doi:10.1103/PhysRevD.78.013004`, `arXiv:0802.0007`.

A   The CMS Collaboration

Yerevan Physics Institute, Yerevan, Armenia
S. Chatrchyan, V. Khachatryan, A.M. Sirunyan, A. Tumasyan

Institut für Hochenergiephysik der OeAW, Wien, Austria
W. Adam, T. Bergauer, M. Dragicevic, J. Erö, C. Fabjan[1], M. Friedl, R. Frühwirth[1], V.M. Ghete, N. Hörmann, J. Hrubec, M. Jeitler[1], W. Kiesenhofer, V. Knünz, M. Krammer[1], I. Krätschmer, D. Liko, I. Mikulec, D. Rabady[2], B. Rahbaran, C. Rohringer, H. Rohringer, R. Schöfbeck, J. Strauss, A. Taurok, W. Treberer-Treberspurg, W. Waltenberger, C.-E. Wulz[1]

National Centre for Particle and High Energy Physics, Minsk, Belarus
V. Mossolov, N. Shumeiko, J. Suarez Gonzalez

Universiteit Antwerpen, Antwerpen, Belgium
S. Alderweireldt, M. Bansal, S. Bansal, T. Cornelis, E.A. De Wolf, X. Janssen, A. Knutsson, S. Luyckx, L. Mucibello, S. Ochesanu, B. Roland, R. Rougny, H. Van Haevermaet, P. Van Mechelen, N. Van Remortel, A. Van Spilbeeck

Vrije Universiteit Brussel, Brussel, Belgium
F. Blekman, S. Blyweert, J. D'Hondt, A. Kalogeropoulos, J. Keaveney, M. Maes, A. Olbrechts, S. Tavernier, W. Van Doninck, P. Van Mulders, G.P. Van Onsem, I. Villella

Université Libre de Bruxelles, Bruxelles, Belgium
B. Clerbaux, G. De Lentdecker, L. Favart, A.P.R. Gay, T. Hreus, A. Léonard, P.E. Marage, A. Mohammadi, L. Perniè, T. Reis, T. Seva, L. Thomas, C. Vander Velde, P. Vanlaer, J. Wang

Ghent University, Ghent, Belgium
V. Adler, K. Beernaert, L. Benucci, A. Cimmino, S. Costantini, S. Dildick, G. Garcia, B. Klein, J. Lellouch, A. Marinov, J. Mccartin, A.A. Ocampo Rios, D. Ryckbosch, M. Sigamani, N. Strobbe, F. Thyssen, M. Tytgat, S. Walsh, E. Yazgan, N. Zaganidis

Université Catholique de Louvain, Louvain-la-Neuve, Belgium
S. Basegmez, C. Beluffi[3], G. Bruno, R. Castello, A. Caudron, L. Ceard, C. Delaere, T. du Pree, D. Favart, L. Forthomme, A. Giammanco[4], J. Hollar, P. Jez, V. Lemaitre, J. Liao, O. Militaru, C. Nuttens, D. Pagano, A. Pin, K. Piotrzkowski, A. Popov[5], M. Selvaggi, J.M. Vizan Garcia

Université de Mons, Mons, Belgium
N. Beliy, T. Caebergs, E. Daubie, G.H. Hammad

Centro Brasileiro de Pesquisas Fisicas, Rio de Janeiro, Brazil
G.A. Alves, M. Correa Martins Junior, T. Martins, M.E. Pol, M.H.G. Souza

Universidade do Estado do Rio de Janeiro, Rio de Janeiro, Brazil
W.L. Aldá Júnior, W. Carvalho, J. Chinellato[6], A. Custódio, E.M. Da Costa, D. De Jesus Damiao, C. De Oliveira Martins, S. Fonseca De Souza, H. Malbouisson, M. Malek, D. Matos Figueiredo, L. Mundim, H. Nogima, W.L. Prado Da Silva, A. Santoro, A. Sznajder, E.J. Tonelli Manganote[6], A. Vilela Pereira

Universidade Estadual Paulista [a], Universidade Federal do ABC [b], São Paulo, Brazil
C.A. Bernardes[b], F.A. Dias[a,7], T.R. Fernandez Perez Tomei[a], E.M. Gregores[b], C. Lagana[a], F. Marinho[a], P.G. Mercadante[b], S.F. Novaes[a], Sandra S. Padula[a]

Institute for Nuclear Research and Nuclear Energy, Sofia, Bulgaria
V. Genchev[2], P. Iaydjiev[2], S. Piperov, M. Rodozov, G. Sultanov, M. Vutova

University of Sofia, Sofia, Bulgaria
A. Dimitrov, R. Hadjiiska, V. Kozhuharov, L. Litov, B. Pavlov, P. Petkov

Institute of High Energy Physics, Beijing, China
J.G. Bian, G.M. Chen, H.S. Chen, C.H. Jiang, D. Liang, S. Liang, X. Meng, J. Tao, J. Wang, X. Wang, Z. Wang, H. Xiao, M. Xu

State Key Laboratory of Nuclear Physics and Technology, Peking University, Beijing, China
C. Asawatangtrakuldee, Y. Ban, Y. Guo, W. Li, S. Liu, Y. Mao, S.J. Qian, H. Teng, D. Wang, L. Zhang, W. Zou

Universidad de Los Andes, Bogota, Colombia
C. Avila, C.A. Carrillo Montoya, J.P. Gomez, B. Gomez Moreno, J.C. Sanabria

Technical University of Split, Split, Croatia
N. Godinovic, D. Lelas, R. Plestina[8], D. Polic, I. Puljak

University of Split, Split, Croatia
Z. Antunovic, M. Kovac

Institute Rudjer Boskovic, Zagreb, Croatia
V. Brigljevic, S. Duric, K. Kadija, J. Luetic, D. Mekterovic, S. Morovic, L. Tikvica

University of Cyprus, Nicosia, Cyprus
A. Attikis, G. Mavromanolakis, J. Mousa, C. Nicolaou, F. Ptochos, P.A. Razis

Charles University, Prague, Czech Republic
M. Finger, M. Finger Jr.

Academy of Scientific Research and Technology of the Arab Republic of Egypt, Egyptian Network of High Energy Physics, Cairo, Egypt
Y. Assran[9], A. Ellithi Kamel[10], M.A. Mahmoud[11], A. Mahrous[12], A. Radi[13,14]

National Institute of Chemical Physics and Biophysics, Tallinn, Estonia
M. Kadastik, M. Müntel, M. Murumaa, M. Raidal, L. Rebane, A. Tiko

Department of Physics, University of Helsinki, Helsinki, Finland
P. Eerola, G. Fedi, M. Voutilainen

Helsinki Institute of Physics, Helsinki, Finland
J. Härkönen, V. Karimäki, R. Kinnunen, M.J. Kortelainen, T. Lampén, K. Lassila-Perini, S. Lehti, T. Lindén, P. Luukka, T. Mäenpää, T. Peltola, E. Tuominen, J. Tuominiemi, E. Tuovinen, L. Wendland

Lappeenranta University of Technology, Lappeenranta, Finland
A. Korpela, T. Tuuva

DSM/IRFU, CEA/Saclay, Gif-sur-Yvette, France
M. Besancon, S. Choudhury, F. Couderc, M. Dejardin, D. Denegri, B. Fabbro, J.L. Faure, F. Ferri, S. Ganjour, A. Givernaud, P. Gras, G. Hamel de Monchenault, P. Jarry, E. Locci, J. Malcles, L. Millischer, A. Nayak, J. Rander, A. Rosowsky, M. Titov

Laboratoire Leprince-Ringuet, Ecole Polytechnique, IN2P3-CNRS, Palaiseau, France
S. Baffioni, F. Beaudette, L. Benhabib, L. Bianchini, M. Bluj[15], P. Busson, C. Charlot, N. Daci, T. Dahms, M. Dalchenko, L. Dobrzynski, A. Florent, R. Granier de Cassagnac, M. Haguenauer, P. Miné, C. Mironov, I.N. Naranjo, M. Nguyen, C. Ochando, P. Paganini, D. Sabes, R. Salerno, Y. Sirois, C. Veelken, A. Zabi

Institut Pluridisciplinaire Hubert Curien, Université de Strasbourg, Université de Haute Alsace Mulhouse, CNRS/IN2P3, Strasbourg, France
J.-L. Agram[16], J. Andrea, D. Bloch, D. Bodin, J.-M. Brom, E.C. Chabert, C. Collard, E. Conte[16], F. Drouhin[16], J.-C. Fontaine[16], D. Gelé, U. Goerlach, C. Goetzmann, P. Juillot, A.-C. Le Bihan, P. Van Hove

Centre de Calcul de l'Institut National de Physique Nucleaire et de Physique des Particules, CNRS/IN2P3, Villeurbanne, France
S. Gadrat

Université de Lyon, Université Claude Bernard Lyon 1, CNRS-IN2P3, Institut de Physique Nucléaire de Lyon, Villeurbanne, France
S. Beauceron, N. Beaupere, G. Boudoul, S. Brochet, J. Chasserat, R. Chierici, D. Contardo, P. Depasse, H. El Mamouni, J. Fay, S. Gascon, M. Gouzevitch, B. Ille, T. Kurca, M. Lethuillier, L. Mirabito, S. Perries, L. Sgandurra, V. Sordini, Y. Tschudi, M. Vander Donckt, P. Verdier, S. Viret

Institute of High Energy Physics and Informatization, Tbilisi State University, Tbilisi, Georgia
Z. Tsamalaidze[17]

RWTH Aachen University, I. Physikalisches Institut, Aachen, Germany
C. Autermann, S. Beranek, B. Calpas, M. Edelhoff, L. Feld, N. Heracleous, O. Hindrichs, K. Klein, A. Ostapchuk, A. Perieanu, F. Raupach, J. Sammet, S. Schael, D. Sprenger, H. Weber, B. Wittmer, V. Zhukov[5]

RWTH Aachen University, III. Physikalisches Institut A, Aachen, Germany
M. Ata, J. Caudron, E. Dietz-Laursonn, D. Duchardt, M. Erdmann, R. Fischer, A. Güth, T. Hebbeker, C. Heidemann, K. Hoepfner, D. Klingebiel, P. Kreuzer, M. Merschmeyer, A. Meyer, M. Olschewski, K. Padeken, P. Papacz, H. Pieta, H. Reithler, S.A. Schmitz, L. Sonnenschein, J. Steggemann, D. Teyssier, S. Thüer, M. Weber

RWTH Aachen University, III. Physikalisches Institut B, Aachen, Germany
V. Cherepanov, Y. Erdogan, G. Flügge, H. Geenen, M. Geisler, W. Haj Ahmad, F. Hoehle, B. Kargoll, T. Kress, Y. Kuessel, J. Lingemann[2], A. Nowack, I.M. Nugent, L. Perchalla, O. Pooth, A. Stahl

Deutsches Elektronen-Synchrotron, Hamburg, Germany
M. Aldaya Martin, I. Asin, N. Bartosik, J. Behr, W. Behrenhoff, U. Behrens, M. Bergholz[18], A. Bethani, K. Borras, A. Burgmeier, A. Cakir, L. Calligaris, A. Campbell, F. Costanza, C. Diez Pardos, S. Dooling, T. Dorland, G. Eckerlin, D. Eckstein, G. Flucke, A. Geiser, I. Glushkov, P. Gunnellini, S. Habib, J. Hauk, G. Hellwig, H. Jung, M. Kasemann, P. Katsas, C. Kleinwort, H. Kluge, M. Krämer, D. Krücker, E. Kuznetsova, W. Lange, J. Leonard, K. Lipka, W. Lohmann[18], B. Lutz, R. Mankel, I. Marfin, I.-A. Melzer-Pellmann, A.B. Meyer, J. Mnich, A. Mussgiller, S. Naumann-Emme, O. Novgorodova, F. Nowak, J. Olzem, H. Perrey, A. Petrukhin, D. Pitzl, R. Placakyte, A. Raspereza, P.M. Ribeiro Cipriano, C. Riedl, E. Ron, M.Ö. Sahin, J. Salfeld-Nebgen, R. Schmidt[18], T. Schoerner-Sadenius, N. Sen, M. Stein, R. Walsh, C. Wissing

University of Hamburg, Hamburg, Germany
V. Blobel, H. Enderle, J. Erfle, U. Gebbert, M. Görner, M. Gosselink, J. Haller, K. Heine, R.S. Höing, G. Kaussen, H. Kirschenmann, R. Klanner, R. Kogler, J. Lange, I. Marchesini, T. Peiffer, N. Pietsch, D. Rathjens, C. Sander, H. Schettler, P. Schleper, E. Schlieckau, A. Schmidt,

M. Schröder, T. Schum, M. Seidel, J. Sibille[19], V. Sola, H. Stadie, G. Steinbrück, J. Thomsen, D. Troendle, L. Vanelderen

Institut für Experimentelle Kernphysik, Karlsruhe, Germany
C. Barth, C. Baus, J. Berger, C. Böser, T. Chwalek, W. De Boer, A. Descroix, A. Dierlamm, M. Feindt, M. Guthoff[2], C. Hackstein, F. Hartmann[2], T. Hauth[2], M. Heinrich, H. Held, K.H. Hoffmann, U. Husemann, I. Katkov[5], J.R. Komaragiri, A. Kornmayer[2], P. Lobelle Pardo, D. Martschei, S. Mueller, Th. Müller, M. Niegel, A. Nürnberg, O. Oberst, J. Ott, G. Quast, K. Rabbertz, F. Ratnikov, S. Röcker, F.-P. Schilling, G. Schott, H.J. Simonis, F.M. Stober, R. Ulrich, J. Wagner-Kuhr, S. Wayand, T. Weiler, M. Zeise

Institute of Nuclear and Particle Physics (INPP),   NCSR Demokritos, Aghia Paraskevi, Greece
G. Anagnostou, G. Daskalakis, T. Geralis, S. Kesisoglou, A. Kyriakis, D. Loukas, A. Markou, C. Markou, E. Ntomari

University of Athens, Athens, Greece
L. Gouskos, T.J. Mertzimekis, A. Panagiotou, N. Saoulidou, E. Stiliaris

University of Ioánnina, Ioánnina, Greece
X. Aslanoglou, I. Evangelou, G. Flouris, C. Foudas, P. Kokkas, N. Manthos, I. Papadopoulos, E. Paradas

KFKI Research Institute for Particle and Nuclear Physics, Budapest, Hungary
G. Bencze, C. Hajdu, P. Hidas, D. Horvath[20], B. Radics, F. Sikler, V. Veszpremi, G. Vesztergombi[21], A.J. Zsigmond

Institute of Nuclear Research ATOMKI, Debrecen, Hungary
N. Beni, S. Czellar, J. Molnar, J. Palinkas, Z. Szillasi

University of Debrecen, Debrecen, Hungary
J. Karancsi, P. Raics, Z.L. Trocsanyi, B. Ujvari

Panjab University, Chandigarh, India
S.B. Beri, V. Bhatnagar, N. Dhingra, R. Gupta, M. Kaur, M.Z. Mehta, M. Mittal, N. Nishu, L.K. Saini, A. Sharma, J.B. Singh

University of Delhi, Delhi, India
Ashok Kumar, Arun Kumar, S. Ahuja, A. Bhardwaj, B.C. Choudhary, S. Malhotra, M. Naimuddin, K. Ranjan, P. Saxena, V. Sharma, R.K. Shivpuri

Saha Institute of Nuclear Physics, Kolkata, India
S. Banerjee, S. Bhattacharya, K. Chatterjee, S. Dutta, B. Gomber, Sa. Jain, Sh. Jain, R. Khurana, A. Modak, S. Mukherjee, D. Roy, S. Sarkar, M. Sharan

Bhabha Atomic Research Centre, Mumbai, India
A. Abdulsalam, D. Dutta, S. Kailas, V. Kumar, A.K. Mohanty[2], L.M. Pant, P. Shukla, A. Topkar

Tata Institute of Fundamental Research - EHEP, Mumbai, India
T. Aziz, R.M. Chatterjee, S. Ganguly, S. Ghosh, M. Guchait[22], A. Gurtu[23], G. Kole, S. Kumar, M. Maity[24], G. Majumder, K. Mazumdar, G.B. Mohanty, B. Parida, K. Sudhakar, N. Wickramage[25]

Tata Institute of Fundamental Research - HECR, Mumbai, India
S. Banerjee, S. Dugad

Institute for Research in Fundamental Sciences (IPM), Tehran, Iran
H. Arfaei[26], H. Bakhshiansohi, S.M. Etesami[27], A. Fahim[26], H. Hesari, A. Jafari, M. Khakzad, M. Mohammadi Najafabadi, S. Paktinat Mehdiabadi, B. Safarzadeh[28], M. Zeinali

University College Dublin, Dublin, Ireland
M. Grunewald

INFN Sezione di Bari [a], Università di Bari [b], Politecnico di Bari [c], Bari, Italy
M. Abbrescia[a,b], L. Barbone[a,b], C. Calabria[a,b], S.S. Chhibra[a,b], A. Colaleo[a], D. Creanza[a,c], N. De Filippis[a,c,2], M. De Palma[a,b], L. Fiore[a], G. Iaselli[a,c], G. Maggi[a,c], M. Maggi[a], B. Marangelli[a,b], S. My[a,c], S. Nuzzo[a,b], N. Pacifico[a], A. Pompili[a,b], G. Pugliese[a,c], G. Selvaggi[a,b], L. Silvestris[a], G. Singh[a,b], R. Venditti[a,b], P. Verwilligen[a], G. Zito[a]

INFN Sezione di Bologna [a], Università di Bologna [b], Bologna, Italy
G. Abbiendi[a], A.C. Benvenuti[a], D. Bonacorsi[a,b], S. Braibant-Giacomelli[a,b], L. Brigliadori[a,b], R. Campanini[a,b], P. Capiluppi[a,b], A. Castro[a,b], F.R. Cavallo[a], M. Cuffiani[a,b], G.M. Dallavalle[a], F. Fabbri[a], A. Fanfani[a,b], D. Fasanella[a,b], P. Giacomelli[a], C. Grandi[a], L. Guiducci[a,b], S. Marcellini[a], G. Masetti[a,2], M. Meneghelli[a,b], A. Montanari[a], F.L. Navarria[a,b], F. Odorici[a], A. Perrotta[a], F. Primavera[a,b], A.M. Rossi[a,b], T. Rovelli[a,b], G.P. Siroli[a,b], N. Tosi[a,b], R. Travaglini[a,b]

INFN Sezione di Catania [a], Università di Catania [b], Catania, Italy
S. Albergo[a,b], M. Chiorboli[a,b], S. Costa[a,b], F. Giordano[a,2], R. Potenza[a,b], A. Tricomi[a,b], C. Tuve[a,b]

INFN Sezione di Firenze [a], Università di Firenze [b], Firenze, Italy
G. Barbagli[a], V. Ciulli[a,b], C. Civinini[a], R. D'Alessandro[a,b], E. Focardi[a,b], S. Frosali[a,b], E. Gallo[a], S. Gonzi[a,b], V. Gori[a,b], P. Lenzi[a,b], M. Meschini[a], S. Paoletti[a], G. Sguazzoni[a], A. Tropiano[a,b]

INFN Laboratori Nazionali di Frascati, Frascati, Italy
L. Benussi, S. Bianco, F. Fabbri, D. Piccolo

INFN Sezione di Genova [a], Università di Genova [b], Genova, Italy
P. Fabbricatore[a], R. Musenich[a], S. Tosi[a,b]

INFN Sezione di Milano-Bicocca [a], Università di Milano-Bicocca [b], Milano, Italy
A. Benaglia[a], F. De Guio[a,b], L. Di Matteo[a,b], S. Fiorendi[a,b], S. Gennai[a], A. Ghezzi[a,b], P. Govoni, M.T. Lucchini[2], S. Malvezzi[a], R.A. Manzoni[a,b,2], A. Martelli[a,b,2], D. Menasce[a], L. Moroni[a], M. Paganoni[a,b], D. Pedrini[a], S. Ragazzi[a,b], N. Redaelli[a], T. Tabarelli de Fatis[a,b]

INFN Sezione di Napoli [a], Università di Napoli 'Federico II' [b], Università della Basilicata (Potenza) [c], Università G. Marconi (Roma) [d], Napoli, Italy
S. Buontempo[a], N. Cavallo[a,c], A. De Cosa[a,b], F. Fabozzi[a,c], A.O.M. Iorio[a,b], L. Lista[a], S. Meola[a,d,2], M. Merola[a], P. Paolucci[a,2]

INFN Sezione di Padova [a], Università di Padova [b], Università di Trento (Trento) [c], Padova, Italy
P. Azzi[a], N. Bacchetta[a], D. Bisello[a,b], A. Branca[a,b], R. Carlin[a,b], P. Checchia[a], T. Dorigo[a], U. Dosselli[a], M. Galanti[a,b,2], F. Gasparini[a,b], U. Gasparini[a,b], P. Giubilato[a,b], A. Gozzelino[a], M. Gulmini[a,29], K. Kanishchev[a,c], S. Lacaprara[a], I. Lazzizzera[a,c], M. Margoni[a,b], G. Maron[a,29], A.T. Meneguzzo[a,b], J. Pazzini[a,b], N. Pozzobon[a,b], P. Ronchese[a,b], F. Simonetto[a,b], E. Torassa[a], M. Tosi[a,b], S. Vanini[a,b], P. Zotto[a,b], A. Zucchetta[a,b], G. Zumerle[a,b]

INFN Sezione di Pavia [a], Università di Pavia [b], Pavia, Italy
M. Gabusi[a,b], S.P. Ratti[a,b], C. Riccardi[a,b], P. Vitulo[a,b]

INFN Sezione di Perugia [a], **Università di Perugia** [b], **Perugia, Italy**
M. Biasini[a,b], G.M. Bilei[a], L. Fanò[a,b], P. Lariccia[a,b], G. Mantovani[a,b], M. Menichelli[a], A. Nappi[a,b†], F. Romeo[a,b], A. Saha[a], A. Santocchia[a,b], A. Spiezia[a,b]

INFN Sezione di Pisa [a], **Università di Pisa** [b], **Scuola Normale Superiore di Pisa** [c], **Pisa, Italy**
K. Androsov[a,30], P. Azzurri[a], G. Bagliesi[a], T. Boccali[a], G. Broccolo[a,c], R. Castaldi[a], R.T. D'Agnolo[a,c,2], R. Dell'Orso[a], F. Fiori[a,c], L. Foà[a,c], A. Giassi[a], A. Kraan[a], F. Ligabue[a,c], T. Lomtadze[a], L. Martini[a,30], A. Messineo[a,b], F. Palla[a], A. Rizzi[a,b], A.T. Serban[a], P. Spagnolo[a], P. Squillacioti[a], R. Tenchini[a], G. Tonelli[a,b], A. Venturi[a], P.G. Verdini[a], C. Vernieri[a,c]

INFN Sezione di Roma [a], **Università di Roma** [b], **Roma, Italy**
L. Barone[a,b], F. Cavallari[a], D. Del Re[a,b], M. Diemoz[a], M. Grassi[a,b,2], E. Longo[a,b], F. Margaroli[a,b], P. Meridiani[a], F. Micheli[a,b], S. Nourbakhsh[a,b], G. Organtini[a,b], R. Paramatti[a], S. Rahatlou[a,b], L. Soffi[a,b]

INFN Sezione di Torino [a], **Università di Torino** [b], **Università del Piemonte Orientale (Novara)** [c], **Torino, Italy**
N. Amapane[a,b], R. Arcidiacono[a,c], S. Argiro[a,b], M. Arneodo[a,c], C. Biino[a], N. Cartiglia[a], S. Casasso[a,b], M. Costa[a,b], N. Demaria[a], C. Mariotti[a], S. Maselli[a], E. Migliore[a,b], V. Monaco[a,b], M. Musich[a], M.M. Obertino[a,c], G. Ortona[a,b], N. Pastrone[a], M. Pelliccioni[a,2], A. Potenza[a,b], A. Romero[a,b], M. Ruspa[a,c], R. Sacchi[a,b], A. Solano[a,b], A. Staiano[a], U. Tamponi[a]

INFN Sezione di Trieste [a], **Università di Trieste** [b], **Trieste, Italy**
S. Belforte[a], V. Candelise[a,b], M. Casarsa[a], F. Cossutti[a,2], G. Della Ricca[a,b], B. Gobbo[a], C. La Licata[a,b], M. Marone[a,b], D. Montanino[a,b], A. Penzo[a], A. Schizzi[a,b], A. Zanetti[a]

Kangwon National University, Chunchon, Korea
T.Y. Kim, S.K. Nam

Kyungpook National University, Daegu, Korea
S. Chang, D.H. Kim, G.N. Kim, J.E. Kim, D.J. Kong, Y.D. Oh, H. Park, D.C. Son

Chonnam National University, Institute for Universe and Elementary Particles, Kwangju, Korea
J.Y. Kim, Zero J. Kim, S. Song

Korea University, Seoul, Korea
S. Choi, D. Gyun, B. Hong, M. Jo, H. Kim, T.J. Kim, K.S. Lee, S.K. Park, Y. Roh

University of Seoul, Seoul, Korea
M. Choi, J.H. Kim, C. Park, I.C. Park, S. Park, G. Ryu

Sungkyunkwan University, Suwon, Korea
Y. Choi, Y.K. Choi, J. Goh, M.S. Kim, E. Kwon, B. Lee, J. Lee, S. Lee, H. Seo, I. Yu

Vilnius University, Vilnius, Lithuania
I. Grigelionis, A. Juodagalvis

Centro de Investigacion y de Estudios Avanzados del IPN, Mexico City, Mexico
H. Castilla-Valdez, E. De La Cruz-Burelo, I. Heredia-de La Cruz[31], R. Lopez-Fernandez, J. Martínez-Ortega, A. Sanchez-Hernandez, L.M. Villasenor-Cendejas

Universidad Iberoamericana, Mexico City, Mexico
S. Carrillo Moreno, F. Vazquez Valencia

Benemerita Universidad Autonoma de Puebla, Puebla, Mexico
H.A. Salazar Ibarguen

Universidad Autónoma de San Luis Potosí, San Luis Potosí, Mexico
E. Casimiro Linares, A. Morelos Pineda, M.A. Reyes-Santos

University of Auckland, Auckland, New Zealand
D. Krofcheck

University of Canterbury, Christchurch, New Zealand
A.J. Bell, P.H. Butler, R. Doesburg, S. Reucroft, H. Silverwood

National Centre for Physics, Quaid-I-Azam University, Islamabad, Pakistan
M. Ahmad, M.I. Asghar, J. Butt, H.R. Hoorani, S. Khalid, W.A. Khan, T. Khurshid, S. Qazi, M.A. Shah, M. Shoaib

National Centre for Nuclear Research, Swierk, Poland
H. Bialkowska, B. Boimska, T. Frueboes, M. Górski, M. Kazana, K. Nawrocki, K. Romanowska-Rybinska, M. Szleper, G. Wrochna, P. Zalewski

Institute of Experimental Physics, Faculty of Physics, University of Warsaw, Warsaw, Poland
G. Brona, K. Bunkowski, M. Cwiok, W. Dominik, K. Doroba, A. Kalinowski, M. Konecki, J. Krolikowski, M. Misiura, W. Wolszczak

Laboratório de Instrumentação e Física Experimental de Partículas, Lisboa, Portugal
N. Almeida, P. Bargassa, A. David, P. Faccioli, P.G. Ferreira Parracho, M. Gallinaro, J. Rodrigues Antunes, J. Seixas[2], J. Varela, P. Vischia

Joint Institute for Nuclear Research, Dubna, Russia
P. Bunin, M. Gavrilenko, I. Golutvin, I. Gorbunov, A. Kamenev, V. Karjavin, V. Konoplyanikov, G. Kozlov, A. Lanev, A. Malakhov, V. Matveev, P. Moisenz, V. Palichik, V. Perelygin, S. Shmatov, N. Skatchkov, V. Smirnov, A. Zarubin

Petersburg Nuclear Physics Institute, Gatchina (St. Petersburg), Russia
S. Evstyukhin, V. Golovtsov, Y. Ivanov, V. Kim, P. Levchenko, V. Murzin, V. Oreshkin, I. Smirnov, V. Sulimov, L. Uvarov, S. Vavilov, A. Vorobyev, An. Vorobyev

Institute for Nuclear Research, Moscow, Russia
Yu. Andreev, A. Dermenev, S. Gninenko, N. Golubev, M. Kirsanov, N. Krasnikov, A. Pashenkov, D. Tlisov, A. Toropin

Institute for Theoretical and Experimental Physics, Moscow, Russia
V. Epshteyn, M. Erofeeva, V. Gavrilov, N. Lychkovskaya, V. Popov, G. Safronov, S. Semenov, A. Spiridonov, V. Stolin, E. Vlasov, A. Zhokin

P.N. Lebedev Physical Institute, Moscow, Russia
V. Andreev, M. Azarkin, I. Dremin, M. Kirakosyan, A. Leonidov, G. Mesyats, S.V. Rusakov, A. Vinogradov

Skobeltsyn Institute of Nuclear Physics, Lomonosov Moscow State University, Moscow, Russia
A. Belyaev, E. Boos, V. Bunichev, M. Dubinin[7], L. Dudko, A. Ershov, A. Gribushin, V. Klyukhin, O. Kodolova, I. Lokhtin, A. Markina, S. Obraztsov, V. Savrin, A. Snigirev

State Research Center of Russian Federation, Institute for High Energy Physics, Protvino, Russia
I. Azhgirey, I. Bayshev, S. Bitioukov, V. Kachanov, A. Kalinin, D. Konstantinov, V. Krychkine, V. Petrov, R. Ryutin, A. Sobol, L. Tourtchanovitch, S. Troshin, N. Tyurin, A. Uzunian, A. Volkov

University of Belgrade, Faculty of Physics and Vinca Institute of Nuclear Sciences, Belgrade, Serbia
P. Adzic[32], M. Ekmedzic, D. Krpic[32], J. Milosevic

Centro de Investigaciones Energéticas Medioambientales y Tecnológicas (CIEMAT), Madrid, Spain
M. Aguilar-Benitez, J. Alcaraz Maestre, C. Battilana, E. Calvo, M. Cerrada, M. Chamizo Llatas[2], N. Colino, B. De La Cruz, A. Delgado Peris, D. Domínguez Vázquez, C. Fernandez Bedoya, J.P. Fernández Ramos, A. Ferrando, J. Flix, M.C. Fouz, P. Garcia-Abia, O. Gonzalez Lopez, S. Goy Lopez, J.M. Hernandez, M.I. Josa, G. Merino, E. Navarro De Martino, J. Puerta Pelayo, A. Quintario Olmeda, I. Redondo, L. Romero, J. Santaolalla, M.S. Soares, C. Willmott

Universidad Autónoma de Madrid, Madrid, Spain
C. Albajar, J.F. de Trocóniz

Universidad de Oviedo, Oviedo, Spain
H. Brun, J. Cuevas, J. Fernandez Menendez, S. Folgueras, I. Gonzalez Caballero, L. Lloret Iglesias, J. Piedra Gomez

Instituto de Física de Cantabria (IFCA), CSIC-Universidad de Cantabria, Santander, Spain
J.A. Brochero Cifuentes, I.J. Cabrillo, A. Calderon, S.H. Chuang, J. Duarte Campderros, M. Fernandez, G. Gomez, J. Gonzalez Sanchez, A. Graziano, C. Jorda, A. Lopez Virto, J. Marco, R. Marco, C. Martinez Rivero, F. Matorras, F.J. Munoz Sanchez, T. Rodrigo, A.Y. Rodríguez-Marrero, A. Ruiz-Jimeno, L. Scodellaro, I. Vila, R. Vilar Cortabitarte

CERN, European Organization for Nuclear Research, Geneva, Switzerland
D. Abbaneo, E. Auffray, G. Auzinger, M. Bachtis, P. Baillon, A.H. Ball, D. Barney, J. Bendavid, J.F. Benitez, C. Bernet[8], G. Bianchi, P. Bloch, A. Bocci, A. Bonato, O. Bondu, C. Botta, H. Breuker, T. Camporesi, G. Cerminara, T. Christiansen, J.A. Coarasa Perez, S. Colafranceschi[33], D. d'Enterria, A. Dabrowski, A. De Roeck, S. De Visscher, S. Di Guida, M. Dobson, N. Dupont-Sagorin, A. Elliott-Peisert, J. Eugster, W. Funk, G. Georgiou, M. Giffels, D. Gigi, K. Gill, D. Giordano, M. Girone, M. Giunta, F. Glege, R. Gomez-Reino Garrido, S. Gowdy, R. Guida, J. Hammer, M. Hansen, P. Harris, C. Hartl, A. Hinzmann, V. Innocente, P. Janot, E. Karavakis, K. Kousouris, K. Krajczar, P. Lecoq, Y.-J. Lee, C. Lourenço, N. Magini, M. Malberti, L. Malgeri, M. Mannelli, L. Masetti, F. Meijers, S. Mersi, E. Meschi, R. Moser, M. Mulders, P. Musella, E. Nesvold, L. Orsini, E. Palencia Cortezon, E. Perez, L. Perrozzi, A. Petrilli, A. Pfeiffer, M. Pierini, M. Pimiä, D. Piparo, M. Plagge, G. Polese, L. Quertenmont, A. Racz, W. Reece, G. Rolandi[34], C. Rovelli[35], M. Rovere, H. Sakulin, F. Santanastasio, C. Schäfer, C. Schwick, I. Segoni, S. Sekmen, A. Sharma, P. Siegrist, P. Silva, M. Simon, P. Sphicas[36], D. Spiga, M. Stoye, A. Tsirou, G.I. Veres[21], J.R. Vlimant, H.K. Wöhri, S.D. Worm[37], W.D. Zeuner

Paul Scherrer Institut, Villigen, Switzerland
W. Bertl, K. Deiters, W. Erdmann, K. Gabathuler, R. Horisberger, Q. Ingram, H.C. Kaestli, S. König, D. Kotlinski, U. Langenegger, D. Renker, T. Rohe

Institute for Particle Physics, ETH Zurich, Zurich, Switzerland
F. Bachmair, L. Bäni, P. Bortignon, M.A. Buchmann, B. Casal, N. Chanon, A. Deisher, G. Dissertori, M. Dittmar, M. Donegà, M. Dünser, P. Eller, K. Freudenreich, C. Grab, D. Hits,

P. Lecomte, W. Lustermann, A.C. Marini, P. Martinez Ruiz del Arbol, N. Mohr, F. Moortgat, C. Nägeli[38], P. Nef, F. Nessi-Tedaldi, F. Pandolfi, L. Pape, F. Pauss, M. Peruzzi, F.J. Ronga, M. Rossini, L. Sala, A.K. Sanchez, A. Starodumov[39], B. Stieger, M. Takahashi, L. Tauscher[†], A. Thea, K. Theofilatos, D. Treille, C. Urscheler, R. Wallny, H.A. Weber

Universität Zürich, Zurich, Switzerland
C. Amsler[40], V. Chiochia, C. Favaro, M. Ivova Rikova, B. Kilminster, B. Millan Mejias, P. Otiougova, P. Robmann, H. Snoek, S. Taroni, S. Tupputi, M. Verzetti

National Central University, Chung-Li, Taiwan
M. Cardaci, K.H. Chen, C. Ferro, C.M. Kuo, S.W. Li, W. Lin, Y.J. Lu, R. Volpe, S.S. Yu

National Taiwan University (NTU), Taipei, Taiwan
P. Bartalini, P. Chang, Y.H. Chang, Y.W. Chang, Y. Chao, K.F. Chen, C. Dietz, U. Grundler, W.-S. Hou, Y. Hsiung, K.Y. Kao, Y.J. Lei, R.-S. Lu, D. Majumder, E. Petrakou, X. Shi, J.G. Shiu, Y.M. Tzeng, M. Wang

Chulalongkorn University, Bangkok, Thailand
B. Asavapibhop, N. Srimanobhas

Cukurova University, Adana, Turkey
A. Adiguzel, M.N. Bakirci[41], S. Cerci[42], C. Dozen, I. Dumanoglu, E. Eskut, S. Girgis, G. Gokbulut, E. Gurpinar, I. Hos, E.E. Kangal, A. Kayis Topaksu, G. Onengut[43], K. Ozdemir, S. Ozturk[41], A. Polatoz, K. Sogut[44], D. Sunar Cerci[42], B. Tali[42], H. Topakli[41], M. Vergili

Middle East Technical University, Physics Department, Ankara, Turkey
I.V. Akin, T. Aliev, B. Bilin, S. Bilmis, M. Deniz, H. Gamsizkan, A.M. Guler, G. Karapinar[45], K. Ocalan, A. Ozpineci, M. Serin, R. Sever, U.E. Surat, M. Yalvac, M. Zeyrek

Bogazici University, Istanbul, Turkey
E. Gülmez, B. Isildak[46], M. Kaya[47], O. Kaya[47], S. Ozkorucuklu[48], N. Sonmez[49]

Istanbul Technical University, Istanbul, Turkey
H. Bahtiyar[50], E. Barlas, K. Cankocak, Y.O. Günaydin[51], F.I. Vardarlı, M. Yücel

National Scientific Center, Kharkov Institute of Physics and Technology, Kharkov, Ukraine
L. Levchuk, P. Sorokin

University of Bristol, Bristol, United Kingdom
J.J. Brooke, E. Clement, D. Cussans, H. Flacher, R. Frazier, J. Goldstein, M. Grimes, G.P. Heath, H.F. Heath, L. Kreczko, S. Metson, D.M. Newbold[37], K. Nirunpong, A. Poll, S. Senkin, V.J. Smith, T. Williams

Rutherford Appleton Laboratory, Didcot, United Kingdom
L. Basso[52], K.W. Bell, A. Belyaev[52], C. Brew, R.M. Brown, D.J.A. Cockerill, J.A. Coughlan, K. Harder, S. Harper, J. Jackson, E. Olaiya, D. Petyt, B.C. Radburn-Smith, C.H. Shepherd-Themistocleous, I.R. Tomalin, W.J. Womersley

Imperial College, London, United Kingdom
R. Bainbridge, O. Buchmuller, D. Burton, D. Colling, N. Cripps, M. Cutajar, P. Dauncey, G. Davies, M. Della Negra, W. Ferguson, J. Fulcher, D. Futyan, A. Gilbert, A. Guneratne Bryer, G. Hall, Z. Hatherell, J. Hays, G. Iles, M. Jarvis, G. Karapostoli, M. Kenzie, R. Lane, R. Lucas[37], L. Lyons, A.-M. Magnan, J. Marrouche, B. Mathias, R. Nandi, J. Nash, A. Nikitenko[39], J. Pela, M. Pesaresi, K. Petridis, M. Pioppi[53], D.M. Raymond, S. Rogerson, A. Rose, C. Seez, P. Sharp[†], A. Sparrow, A. Tapper, M. Vazquez Acosta, T. Virdee, S. Wakefield, N. Wardle, T. Whyntie

Brunel University, Uxbridge, United Kingdom
M. Chadwick, J.E. Cole, P.R. Hobson, A. Khan, P. Kyberd, D. Leggat, D. Leslie, W. Martin, I.D. Reid, P. Symonds, L. Teodorescu, M. Turner

Baylor University, Waco, USA
J. Dittmann, K. Hatakeyama, A. Kasmi, H. Liu, T. Scarborough

The University of Alabama, Tuscaloosa, USA
O. Charaf, S.I. Cooper, C. Henderson, P. Rumerio

Boston University, Boston, USA
A. Avetisyan, T. Bose, C. Fantasia, A. Heister, P. Lawson, D. Lazic, J. Rohlf, D. Sperka, J. St. John, L. Sulak

Brown University, Providence, USA
J. Alimena, S. Bhattacharya, G. Christopher, D. Cutts, Z. Demiragli, A. Ferapontov, A. Garabedian, U. Heintz, G. Kukartsev, E. Laird, G. Landsberg, M. Luk, M. Narain, M. Segala, T. Sinthuprasith, T. Speer

University of California, Davis, Davis, USA
R. Breedon, G. Breto, M. Calderon De La Barca Sanchez, S. Chauhan, M. Chertok, J. Conway, R. Conway, P.T. Cox, R. Erbacher, M. Gardner, R. Houtz, W. Ko, A. Kopecky, R. Lander, O. Mall, T. Miceli, R. Nelson, D. Pellett, F. Ricci-Tam, B. Rutherford, M. Searle, J. Smith, M. Squires, M. Tripathi, S. Wilbur, R. Yohay

University of California, Los Angeles, USA
V. Andreev, D. Cline, R. Cousins, S. Erhan, P. Everaerts, C. Farrell, M. Felcini, J. Hauser, M. Ignatenko, C. Jarvis, G. Rakness, P. Schlein[†], E. Takasugi, P. Traczyk, V. Valuev, M. Weber

University of California, Riverside, Riverside, USA
J. Babb, R. Clare, M.E. Dinardo, J. Ellison, J.W. Gary, G. Hanson, H. Liu, O.R. Long, A. Luthra, H. Nguyen, S. Paramesvaran, J. Sturdy, S. Sumowidagdo, R. Wilken, S. Wimpenny

University of California, San Diego, La Jolla, USA
W. Andrews, J.G. Branson, G.B. Cerati, S. Cittolin, D. Evans, A. Holzner, R. Kelley, M. Lebourgeois, J. Letts, I. Macneill, B. Mangano, S. Padhi, C. Palmer, G. Petrucciani, M. Pieri, M. Sani, V. Sharma, S. Simon, E. Sudano, M. Tadel, Y. Tu, A. Vartak, S. Wasserbaech[54], F. Würthwein, A. Yagil, J. Yoo

University of California, Santa Barbara, Santa Barbara, USA
D. Barge, R. Bellan, C. Campagnari, M. D'Alfonso, T. Danielson, K. Flowers, P. Geffert, C. George, F. Golf, J. Incandela, C. Justus, P. Kalavase, D. Kovalskyi, V. Krutelyov, S. Lowette, R. Magaña Villalba, N. Mccoll, V. Pavlunin, J. Ribnik, J. Richman, R. Rossin, D. Stuart, W. To, C. West

California Institute of Technology, Pasadena, USA
A. Apresyan, A. Bornheim, J. Bunn, Y. Chen, E. Di Marco, J. Duarte, D. Kcira, Y. Ma, A. Mott, H.B. Newman, C. Rogan, M. Spiropulu, V. Timciuc, J. Veverka, R. Wilkinson, S. Xie, Y. Yang, R.Y. Zhu

Carnegie Mellon University, Pittsburgh, USA
V. Azzolini, A. Calamba, R. Carroll, T. Ferguson, Y. Iiyama, D.W. Jang, Y.F. Liu, M. Paulini, J. Russ, H. Vogel, I. Vorobiev

University of Colorado at Boulder, Boulder, USA
J.P. Cumalat, B.R. Drell, W.T. Ford, A. Gaz, E. Luiggi Lopez, U. Nauenberg, J.G. Smith, K. Stenson, K.A. Ulmer, S.R. Wagner

Cornell University, Ithaca, USA
J. Alexander, A. Chatterjee, N. Eggert, L.K. Gibbons, W. Hopkins, A. Khukhunaishvili, B. Kreis, N. Mirman, G. Nicolas Kaufman, J.R. Patterson, A. Ryd, E. Salvati, W. Sun, W.D. Teo, J. Thom, J. Thompson, J. Tucker, Y. Weng, L. Winstrom, P. Wittich

Fairfield University, Fairfield, USA
D. Winn

Fermi National Accelerator Laboratory, Batavia, USA
S. Abdullin, M. Albrow, J. Anderson, G. Apollinari, L.A.T. Bauerdick, A. Beretvas, J. Berryhill, P.C. Bhat, K. Burkett, J.N. Butler, V. Chetluru, H.W.K. Cheung, F. Chlebana, S. Cihangir, V.D. Elvira, I. Fisk, J. Freeman, Y. Gao, E. Gottschalk, L. Gray, D. Green, O. Gutsche, D. Hare, R.M. Harris, J. Hirschauer, B. Hooberman, S. Jindariani, M. Johnson, U. Joshi, B. Klima, S. Kunori, S. Kwan, C. Leonidopoulos[55], J. Linacre, D. Lincoln, R. Lipton, J. Lykken, K. Maeshima, J.M. Marraffino, V.I. Martinez Outschoorn, S. Maruyama, D. Mason, P. McBride, K. Mishra, S. Mrenna, Y. Musienko[56], C. Newman-Holmes, V. O'Dell, O. Prokofyev, N. Ratnikova, E. Sexton-Kennedy, S. Sharma, W.J. Spalding, L. Spiegel, L. Taylor, S. Tkaczyk, N.V. Tran, L. Uplegger, E.W. Vaandering, R. Vidal, J. Whitmore, W. Wu, F. Yang, J.C. Yun

University of Florida, Gainesville, USA
D. Acosta, P. Avery, D. Bourilkov, M. Chen, T. Cheng, S. Das, M. De Gruttola, G.P. Di Giovanni, D. Dobur, A. Drozdetskiy, R.D. Field, M. Fisher, Y. Fu, I.K. Furic, J. Hugon, B. Kim, J. Konigsberg, A. Korytov, A. Kropivnitskaya, T. Kypreos, J.F. Low, K. Matchev, P. Milenovic[57], G. Mitselmakher, L. Muniz, R. Remington, A. Rinkevicius, N. Skhirtladze, M. Snowball, J. Yelton, M. Zakaria

Florida International University, Miami, USA
V. Gaultney, S. Hewamanage, L.M. Lebolo, S. Linn, P. Markowitz, G. Martinez, J.L. Rodriguez

Florida State University, Tallahassee, USA
T. Adams, A. Askew, J. Bochenek, J. Chen, B. Diamond, S.V. Gleyzer, J. Haas, S. Hagopian, V. Hagopian, K.F. Johnson, H. Prosper, V. Veeraraghavan, M. Weinberg

Florida Institute of Technology, Melbourne, USA
M.M. Baarmand, B. Dorney, M. Hohlmann, H. Kalakhety, F. Yumiceva

University of Illinois at Chicago (UIC), Chicago, USA
M.R. Adams, L. Apanasevich, V.E. Bazterra, R.R. Betts, I. Bucinskaite, J. Callner, R. Cavanaugh, O. Evdokimov, L. Gauthier, C.E. Gerber, D.J. Hofman, S. Khalatyan, P. Kurt, F. Lacroix, D.H. Moon, C. O'Brien, C. Silkworth, D. Strom, P. Turner, N. Varelas

The University of Iowa, Iowa City, USA
U. Akgun, E.A. Albayrak[50], B. Bilki[58], W. Clarida, K. Dilsiz, F. Duru, S. Griffiths, J.-P. Merlo, H. Mermerkaya[59], A. Mestvirishvili, A. Moeller, J. Nachtman, C.R. Newsom, H. Ogul, Y. Onel, F. Ozok[50], S. Sen, P. Tan, E. Tiras, J. Wetzel, T. Yetkin[60], K. Yi

Johns Hopkins University, Baltimore, USA
B.A. Barnett, B. Blumenfeld, S. Bolognesi, D. Fehling, G. Giurgiu, A.V. Gritsan, Z.J. Guo, G. Hu, P. Maksimovic, M. Swartz, A. Whitbeck

The University of Kansas, Lawrence, USA
P. Baringer, A. Bean, G. Benelli, R.P. Kenny III, M. Murray, D. Noonan, S. Sanders, R. Stringer, J.S. Wood

Kansas State University, Manhattan, USA
A.F. Barfuss, I. Chakaberia, A. Ivanov, S. Khalil, M. Makouski, Y. Maravin, S. Shrestha, I. Svintradze

Lawrence Livermore National Laboratory, Livermore, USA
J. Gronberg, D. Lange, F. Rebassoo, D. Wright

University of Maryland, College Park, USA
A. Baden, B. Calvert, S.C. Eno, J.A. Gomez, N.J. Hadley, R.G. Kellogg, T. Kolberg, Y. Lu, M. Marionneau, A.C. Mignerey, K. Pedro, A. Peterman, A. Skuja, J. Temple, M.B. Tonjes, S.C. Tonwar

Massachusetts Institute of Technology, Cambridge, USA
A. Apyan, G. Bauer, W. Busza, E. Butz, I.A. Cali, M. Chan, V. Dutta, G. Gomez Ceballos, M. Goncharov, Y. Kim, M. Klute, Y.S. Lai, A. Levin, P.D. Luckey, T. Ma, S. Nahn, C. Paus, D. Ralph, C. Roland, G. Roland, G.S.F. Stephans, F. Stöckli, K. Sumorok, K. Sung, D. Velicanu, R. Wolf, B. Wyslouch, M. Yang, Y. Yilmaz, A.S. Yoon, M. Zanetti, V. Zhukova

University of Minnesota, Minneapolis, USA
B. Dahmes, A. De Benedetti, G. Franzoni, A. Gude, J. Haupt, S.C. Kao, K. Klapoetke, Y. Kubota, J. Mans, N. Pastika, R. Rusack, M. Sasseville, A. Singovsky, N. Tambe, J. Turkewitz

University of Mississippi, Oxford, USA
L.M. Cremaldi, R. Kroeger, L. Perera, R. Rahmat, D.A. Sanders, D. Summers

University of Nebraska-Lincoln, Lincoln, USA
E. Avdeeva, K. Bloom, S. Bose, D.R. Claes, A. Dominguez, M. Eads, R. Gonzalez Suarez, J. Keller, I. Kravchenko, J. Lazo-Flores, S. Malik, F. Meier, G.R. Snow

State University of New York at Buffalo, Buffalo, USA
J. Dolen, A. Godshalk, I. Iashvili, S. Jain, A. Kharchilava, A. Kumar, S. Rappoccio, Z. Wan

Northeastern University, Boston, USA
G. Alverson, E. Barberis, D. Baumgartel, M. Chasco, J. Haley, A. Massironi, D. Nash, T. Orimoto, D. Trocino, D. Wood, J. Zhang

Northwestern University, Evanston, USA
A. Anastassov, K.A. Hahn, A. Kubik, L. Lusito, N. Mucia, N. Odell, B. Pollack, A. Pozdnyakov, M. Schmitt, S. Stoynev, M. Velasco, S. Won

University of Notre Dame, Notre Dame, USA
D. Berry, A. Brinkerhoff, K.M. Chan, M. Hildreth, C. Jessop, D.J. Karmgard, J. Kolb, K. Lannon, W. Luo, S. Lynch, N. Marinelli, D.M. Morse, T. Pearson, M. Planer, R. Ruchti, J. Slaunwhite, N. Valls, M. Wayne, M. Wolf

The Ohio State University, Columbus, USA
L. Antonelli, B. Bylsma, L.S. Durkin, C. Hill, R. Hughes, K. Kotov, T.Y. Ling, D. Puigh, M. Rodenburg, G. Smith, C. Vuosalo, G. Williams, B.L. Winer, H. Wolfe

Princeton University, Princeton, USA
E. Berry, P. Elmer, V. Halyo, P. Hebda, J. Hegeman, A. Hunt, P. Jindal, S.A. Koay, D. Lopes

Pegna, P. Lujan, D. Marlow, T. Medvedeva, M. Mooney, J. Olsen, P. Piroué, X. Quan, A. Raval, H. Saka, D. Stickland, C. Tully, J.S. Werner, S.C. Zenz, A. Zuranski

University of Puerto Rico, Mayaguez, USA
E. Brownson, A. Lopez, H. Mendez, J.E. Ramirez Vargas

Purdue University, West Lafayette, USA
E. Alagoz, D. Benedetti, G. Bolla, D. Bortoletto, M. De Mattia, A. Everett, Z. Hu, M. Jones, K. Jung, O. Koybasi, M. Kress, N. Leonardo, V. Maroussov, P. Merkel, D.H. Miller, N. Neumeister, I. Shipsey, D. Silvers, A. Svyatkovskiy, M. Vidal Marono, F. Wang, L. Xu, H.D. Yoo, J. Zablocki, Y. Zheng

Purdue University Calumet, Hammond, USA
S. Guragain, N. Parashar

Rice University, Houston, USA
A. Adair, B. Akgun, K.M. Ecklund, F.J.M. Geurts, W. Li, B.P. Padley, R. Redjimi, J. Roberts, J. Zabel

University of Rochester, Rochester, USA
B. Betchart, A. Bodek, R. Covarelli, P. de Barbaro, R. Demina, Y. Eshaq, T. Ferbel, A. Garcia-Bellido, P. Goldenzweig, J. Han, A. Harel, D.C. Miner, G. Petrillo, D. Vishnevskiy, M. Zielinski

The Rockefeller University, New York, USA
A. Bhatti, R. Ciesielski, L. Demortier, K. Goulianos, G. Lungu, S. Malik, C. Mesropian

Rutgers, The State University of New Jersey, Piscataway, USA
S. Arora, A. Barker, J.P. Chou, C. Contreras-Campana, E. Contreras-Campana, D. Duggan, D. Ferencek, Y. Gershtein, R. Gray, E. Halkiadakis, D. Hidas, A. Lath, S. Panwalkar, M. Park, R. Patel, V. Rekovic, J. Robles, K. Rose, S. Salur, S. Schnetzer, C. Seitz, S. Somalwar, R. Stone, S. Thomas, M. Walker

University of Tennessee, Knoxville, USA
G. Cerizza, M. Hollingsworth, S. Spanier, Z.C. Yang, A. York

Texas A&M University, College Station, USA
R. Eusebi, W. Flanagan, J. Gilmore, T. Kamon[61], V. Khotilovich, R. Montalvo, I. Osipenkov, Y. Pakhotin, A. Perloff, J. Roe, A. Safonov, T. Sakuma, I. Suarez, A. Tatarinov, D. Toback

Texas Tech University, Lubbock, USA
N. Akchurin, J. Damgov, C. Dragoiu, P.R. Dudero, C. Jeong, K. Kovitanggoon, S.W. Lee, T. Libeiro, I. Volobouev

Vanderbilt University, Nashville, USA
E. Appelt, A.G. Delannoy, S. Greene, A. Gurrola, W. Johns, C. Maguire, Y. Mao, A. Melo, M. Sharma, P. Sheldon, B. Snook, S. Tuo, J. Velkovska

University of Virginia, Charlottesville, USA
M.W. Arenton, S. Boutle, B. Cox, B. Francis, J. Goodell, R. Hirosky, A. Ledovskoy, C. Lin, C. Neu, J. Wood

Wayne State University, Detroit, USA
S. Gollapinni, R. Harr, P.E. Karchin, C. Kottachchi Kankanamge Don, P. Lamichhane, A. Sakharov

University of Wisconsin, Madison, USA
M. Anderson, D.A. Belknap, L. Borrello, D. Carlsmith, M. Cepeda, S. Dasu, E. Friis, K.S. Grogg, M. Grothe, R. Hall-Wilton, M. Herndon, A. Hervé, K. Kaadze, P. Klabbers, J. Klukas, A. Lanaro, C. Lazaridis, R. Loveless, A. Mohapatra, M.U. Mozer, I. Ojalvo, G.A. Pierro, I. Ross, A. Savin, W.H. Smith, J. Swanson

†: Deceased
1: Also at Vienna University of Technology, Vienna, Austria
2: Also at CERN, European Organization for Nuclear Research, Geneva, Switzerland
3: Also at Institut Pluridisciplinaire Hubert Curien, Université de Strasbourg, Université de Haute Alsace Mulhouse, CNRS/IN2P3, Strasbourg, France
4: Also at National Institute of Chemical Physics and Biophysics, Tallinn, Estonia
5: Also at Skobeltsyn Institute of Nuclear Physics, Lomonosov Moscow State University, Moscow, Russia
6: Also at Universidade Estadual de Campinas, Campinas, Brazil
7: Also at California Institute of Technology, Pasadena, USA
8: Also at Laboratoire Leprince-Ringuet, Ecole Polytechnique, IN2P3-CNRS, Palaiseau, France
9: Also at Suez Canal University, Suez, Egypt
10: Also at Cairo University, Cairo, Egypt
11: Also at Fayoum University, El-Fayoum, Egypt
12: Also at Helwan University, Cairo, Egypt
13: Also at British University in Egypt, Cairo, Egypt
14: Now at Ain Shams University, Cairo, Egypt
15: Also at National Centre for Nuclear Research, Swierk, Poland
16: Also at Université de Haute Alsace, Mulhouse, France
17: Also at Joint Institute for Nuclear Research, Dubna, Russia
18: Also at Brandenburg University of Technology, Cottbus, Germany
19: Also at The University of Kansas, Lawrence, USA
20: Also at Institute of Nuclear Research ATOMKI, Debrecen, Hungary
21: Also at Eötvös Loránd University, Budapest, Hungary
22: Also at Tata Institute of Fundamental Research - HECR, Mumbai, India
23: Now at King Abdulaziz University, Jeddah, Saudi Arabia
24: Also at University of Visva-Bharati, Santiniketan, India
25: Also at University of Ruhuna, Matara, Sri Lanka
26: Also at Sharif University of Technology, Tehran, Iran
27: Also at Isfahan University of Technology, Isfahan, Iran
28: Also at Plasma Physics Research Center, Science and Research Branch, Islamic Azad University, Tehran, Iran
29: Also at Laboratori Nazionali di Legnaro dell' INFN, Legnaro, Italy
30: Also at Università degli Studi di Siena, Siena, Italy
31: Also at Universidad Michoacana de San Nicolas de Hidalgo, Morelia, Mexico
32: Also at Faculty of Physics, University of Belgrade, Belgrade, Serbia
33: Also at Facoltà Ingegneria, Università di Roma, Roma, Italy
34: Also at Scuola Normale e Sezione dell'INFN, Pisa, Italy
35: Also at INFN Sezione di Roma, Roma, Italy
36: Also at University of Athens, Athens, Greece
37: Also at Rutherford Appleton Laboratory, Didcot, United Kingdom
38: Also at Paul Scherrer Institut, Villigen, Switzerland
39: Also at Institute for Theoretical and Experimental Physics, Moscow, Russia
40: Also at Albert Einstein Center for Fundamental Physics, Bern, Switzerland

41: Also at Gaziosmanpasa University, Tokat, Turkey
42: Also at Adiyaman University, Adiyaman, Turkey
43: Also at Cag University, Mersin, Turkey
44: Also at Mersin University, Mersin, Turkey
45: Also at Izmir Institute of Technology, Izmir, Turkey
46: Also at Ozyegin University, Istanbul, Turkey
47: Also at Kafkas University, Kars, Turkey
48: Also at Suleyman Demirel University, Isparta, Turkey
49: Also at Ege University, Izmir, Turkey
50: Also at Mimar Sinan University, Istanbul, Istanbul, Turkey
51: Also at Kahramanmaras Sütcü Imam University, Kahramanmaras, Turkey
52: Also at School of Physics and Astronomy, University of Southampton, Southampton, United Kingdom
53: Also at INFN Sezione di Perugia; Università di Perugia, Perugia, Italy
54: Also at Utah Valley University, Orem, USA
55: Now at University of Edinburgh, Scotland, Edinburgh, United Kingdom
56: Also at Institute for Nuclear Research, Moscow, Russia
57: Also at University of Belgrade, Faculty of Physics and Vinca Institute of Nuclear Sciences, Belgrade, Serbia
58: Also at Argonne National Laboratory, Argonne, USA
59: Also at Erzincan University, Erzincan, Turkey
60: Also at Yildiz Technical University, Istanbul, Turkey
61: Also at Kyungpook National University, Daegu, Korea